

# Inverse problems: theory, applications, and computational solution

Samuli Siltanen

Department of Mathematics and Statistics  
University of Helsinki, Finland  
[samuli.siltanen@helsinki.fi](mailto:samuli.siltanen@helsinki.fi)  
[www.siltanen-research.net](http://www.siltanen-research.net)

Tokyo University of Science

January 21, 2016





# Finnish Centre of Excellence in Inverse Problems Research



# This my industrial-academic background



1999: PhD, Helsinki University of Technology, Finland



2000: R&D scientist at Instrumentarium Imaging



2002: Postdoc at Gunma University, Japan



2004: R&D scientist at GE Healthcare



2005: R&D scientist at Palodex Group



2006: Professor, Tampere University of Technology, Finland



2009: Professor, University of Helsinki, Finland

# Outline

## Inverse problems and ill-posedness

### X-ray tomography

Mathematical model of X-ray attenuation

Tomographic imaging with sparse data

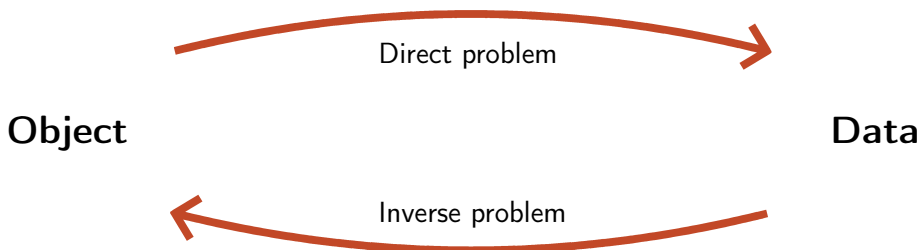
Regularized inversion

Industrial case study: low-dose 3D dental X-ray imaging

Conclusion: linear and nonlinear inverse problems

**Direct problem:** *given object, determine data*

**Inverse problem:** *given noisy data, recover object*



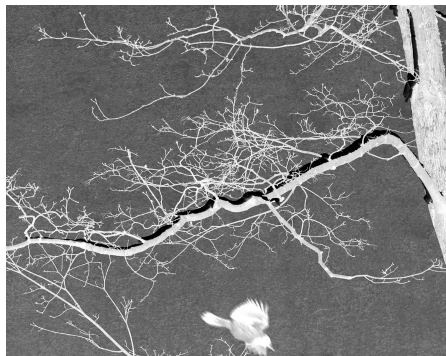
**Direct problem:** *given object, determine data*

**Inverse problem:** *given noisy data, recover object*

**Object** (positive photograph)



**Data** (negative photograph)



**Forward map:** subtraction from a constant

**Direct problem:** *given object, determine data*

**Inverse problem:** *given noisy data, recover object*

**Object** (sharp photograph)



**Data** (blurred photograph)



Forward map: convolution operator with smooth kernel

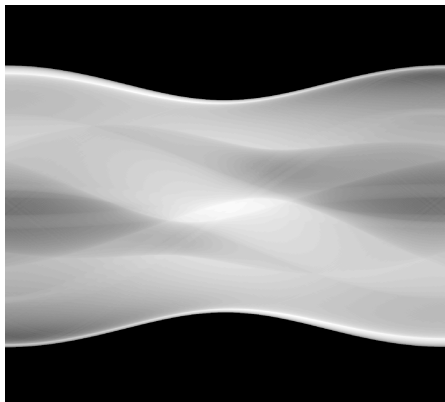
**Direct problem:** *given object, determine data*

**Inverse problem:** *given noisy data, recover object*

**Object** (X-ray attenuation)



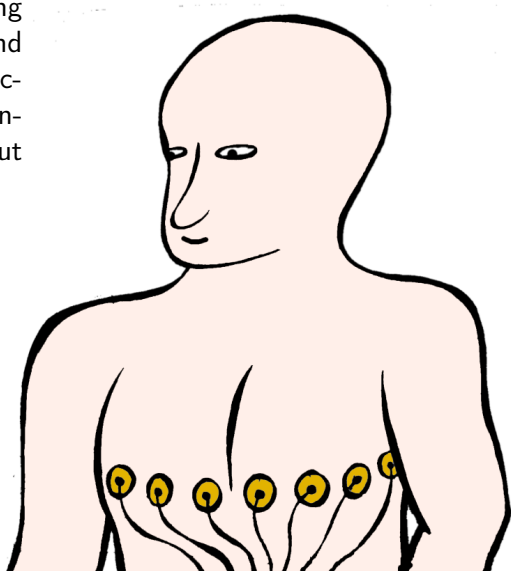
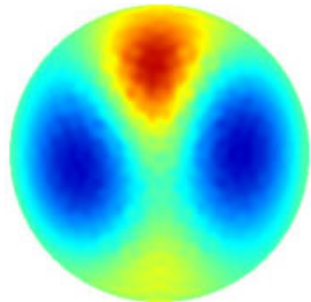
**Data** (sinogram)



**Forward map:** discrete Radon transform

## In Electrical Impedance Tomography (EIT), currents are fed and voltages measured

Medical applications: monitoring cardiac activity, lung function, and pulmonary perfusion. Also, electrocardiography (ECG) can be enhanced using knowledge about conductivity distribution.



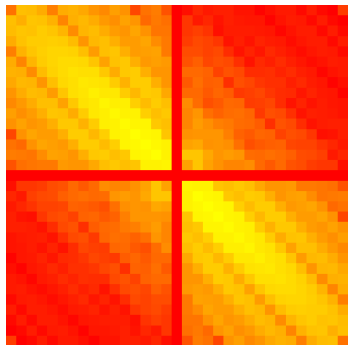
**Direct problem:** *given object, determine data*

**Inverse problem:** *given noisy data, recover object*

**Object** (conductivity)

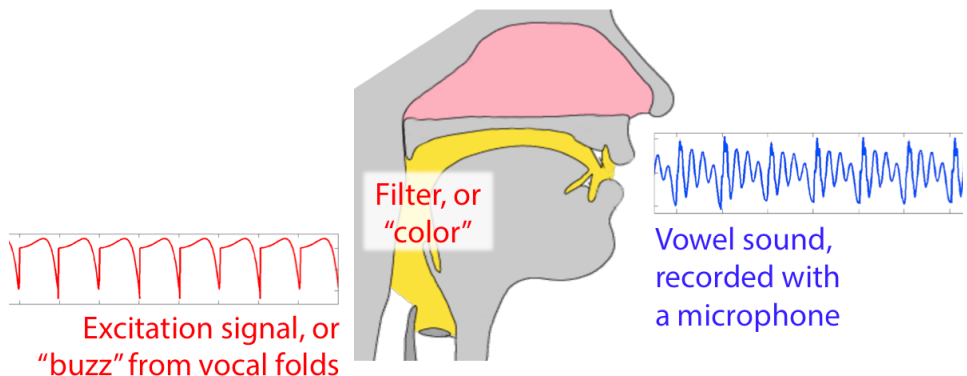


**Data** (voltage-to-current map)



Forward map: electrical boundary measurements

A vowel sound consists of two structural parts:  
excitation and vocal tract filter



**Direct problem:** *given object, determine data*

**Inverse problem:** *given noisy data, recover object*

In glottal inverse filtering (GIF), the data is a **vowel sound** recorded using a microphone. The aim is to reconstruct the **excitation signal** and the **filter**.

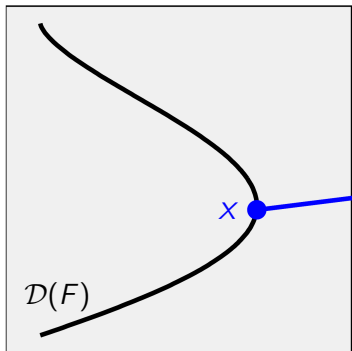
GIF has important applications in

- ▶ Computer-generated speech (think Stephen Hawking),
- ▶ Speech recognition (think Apple's Siri).

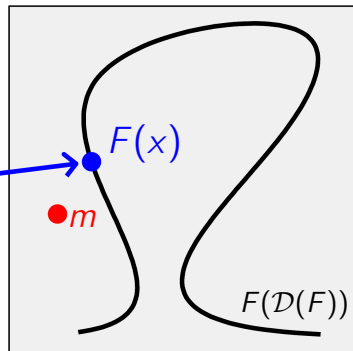
Forward map: bilinear convolution operator

**Inverse problem = interpretation of an indirect measurement modelled by a forward map  $F$**

Model space  $X$



Data space  $Y$



Consider the measurement model  $m = F(x) + \varepsilon$ . We want to know  $x$ , but all we can do is measure  $m$  that depends indirectly on  $x$ . Moreover, the measurement is corrupted with noise  $\varepsilon$ .

# III-posed inverse problems are defined as opposites of well-posed direct problems



Hadamard (1903): a problem is well-posed if the following conditions hold.

1. A solution exists,
2. The solution is unique,
3. The solution depends continuously on the input.

Well-posed direct problem:

Input  $x$ , find infinite-precision data  $F(x)$ .

III-posed inverse problem:

Input noisy data  $m = F(x) + \varepsilon$ , recover  $x$ .

The solution of an inverse problem is a *set of instructions* for recovering  $\times$  stably from  $m$

Those instructions need to be

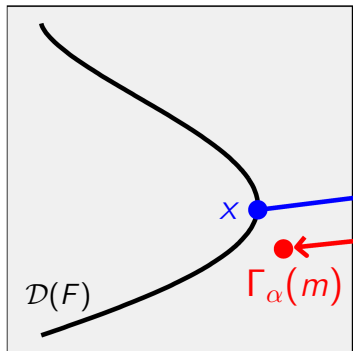
- (i) backed up by rigorous mathematical theory, and
- (ii) implementable as an effective computational algorithm.

Ill-posed inverse problems are very sensitive to modelling errors and measurement noise. Therefore, the solution needs *a priori* information about the unknown in addition to measurement data.

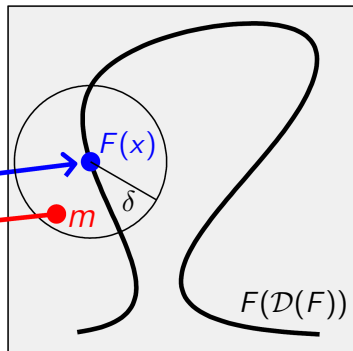
Such *a priori* information is used by designing and implementing a regularization strategy  $\Gamma_\alpha$ .

Regularization means constructing a continuous map  $\Gamma_\alpha : Y \rightarrow X$  that inverts  $F$  approximately

Model space  $X$



Data space  $Y$



Here  $\Gamma_{\alpha(\delta)}(m)$  should approach  $x$  along a stable path as  $\delta \rightarrow 0$ .

# Outline

Inverse problems and ill-posedness

## X-ray tomography

Mathematical model of X-ray attenuation

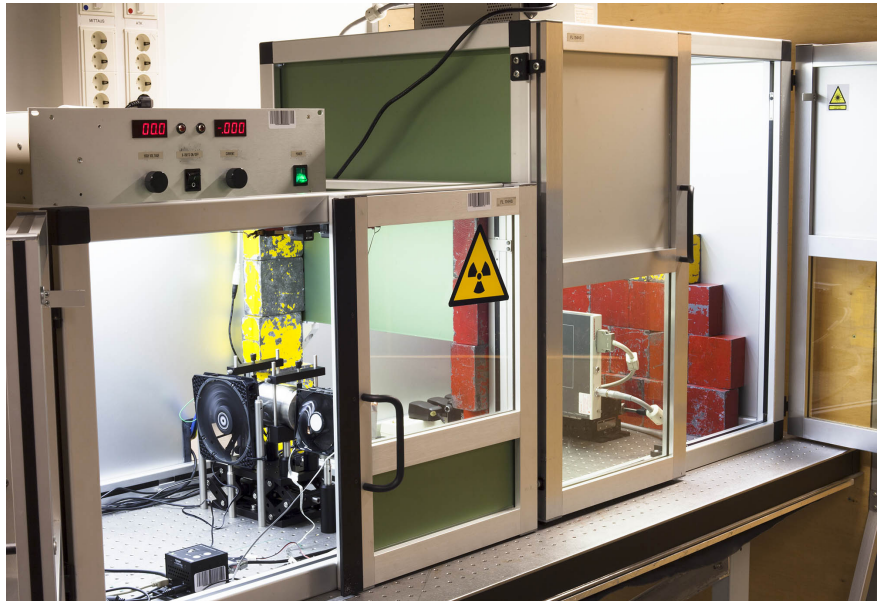
Tomographic imaging with sparse data

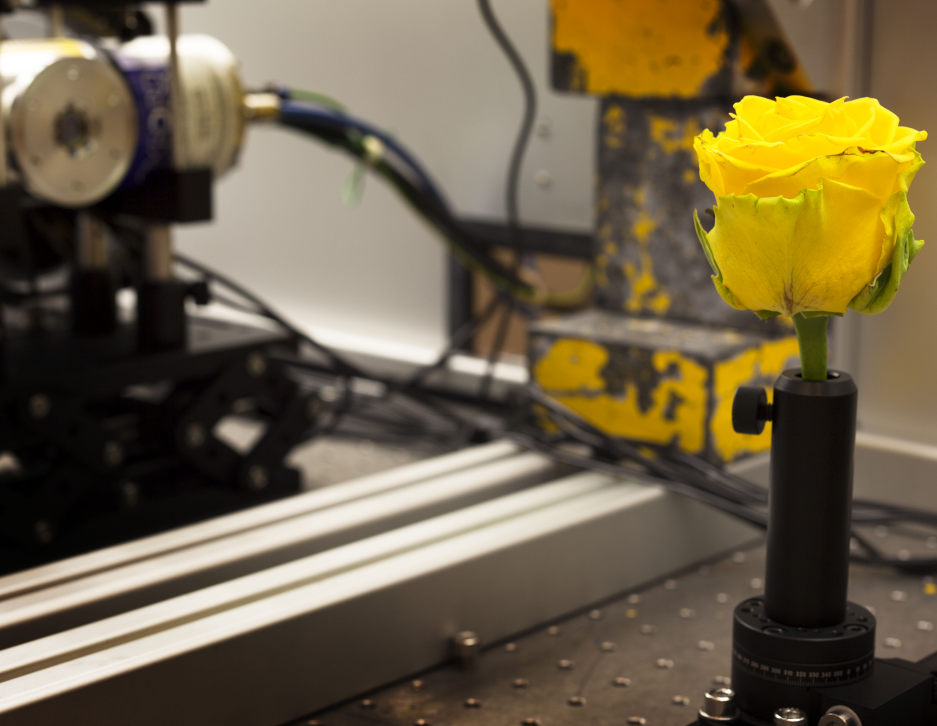
Regularized inversion

Industrial case study: low-dose 3D dental X-ray imaging

Conclusion: linear and nonlinear inverse problems

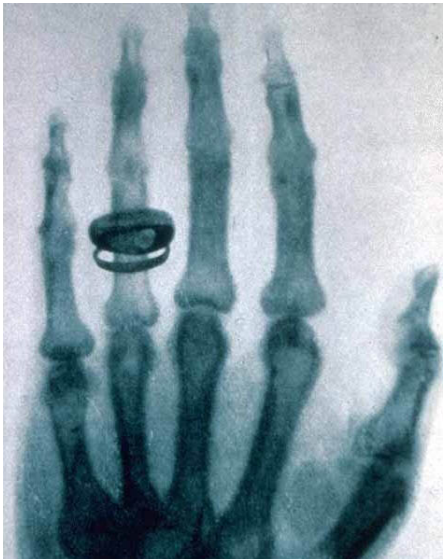
# This is my new X-ray laboratory at University of Helsinki







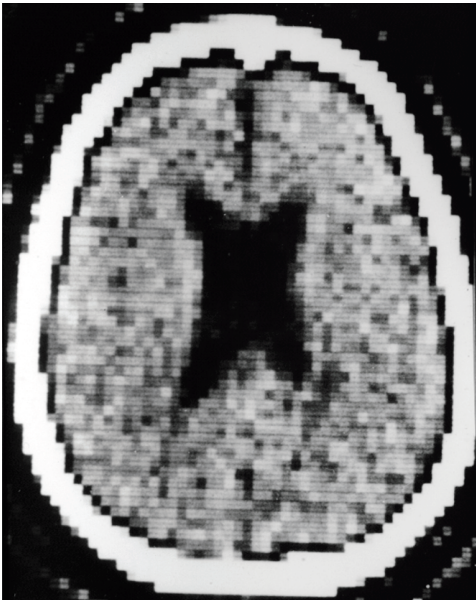
**Wilhelm Conrad Röntgen invented X-rays and was awarded the first Nobel Prize in Physics in 1901**



# Godfrey Hounsfield and Allan McLeod Cormack developed X-ray tomography



Hounsfield (top) and Cormack received Nobel prizes in 1979.



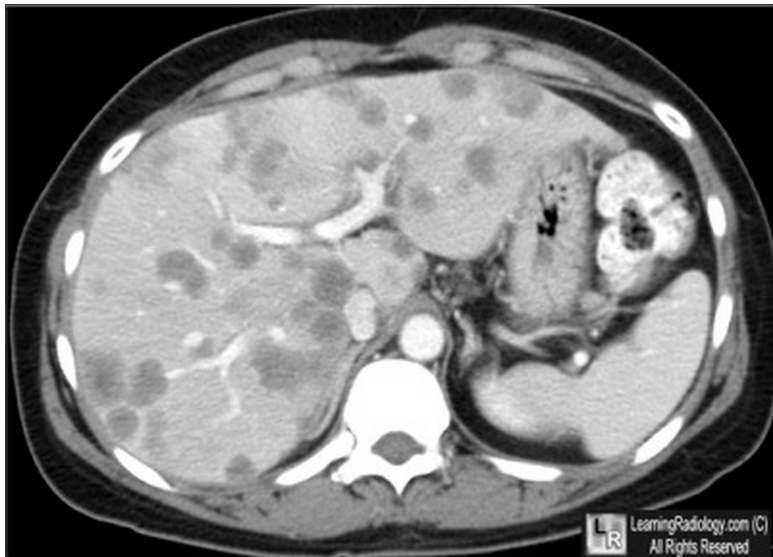
**Reconstruction of a function from its line integrals  
was first invented by Johann Radon in 1917**



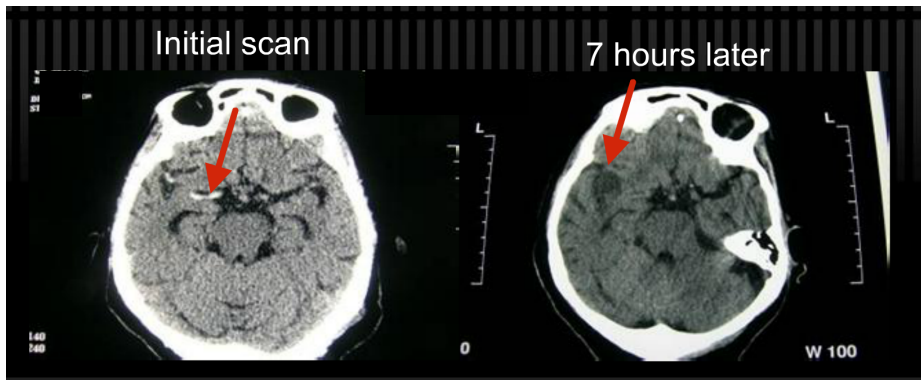
$$f(P) = -\frac{1}{\pi} \int_0^\infty \frac{d\overline{F}_p(q)}{q}$$

Johann Radon (1887-1956)

# Contrast-enhanced CT of abdomen, showing liver metastases

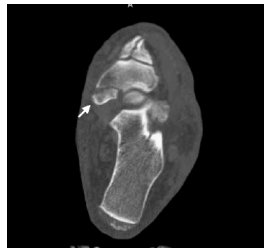


# Head CT can be used for detecting and monitoring brain hemorrhage

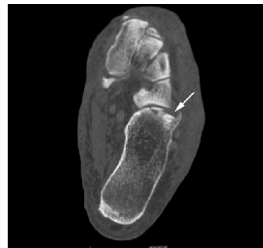


# Unusual variant of the Nutcracker Fracture of the calcaneus and tarsal navicular

Axial slice of the right foot



Another axial slice



Sagittal slice



3D render



[Gajendran, Yoo & Hunter, Radiology Case Reports 3 (2008)]

# Outline

Inverse problems and ill-posedness

X-ray tomography

Mathematical model of X-ray attenuation

Tomographic imaging with sparse data

Regularized inversion

Industrial case study: low-dose 3D dental X-ray imaging

Conclusion: linear and nonlinear inverse problems

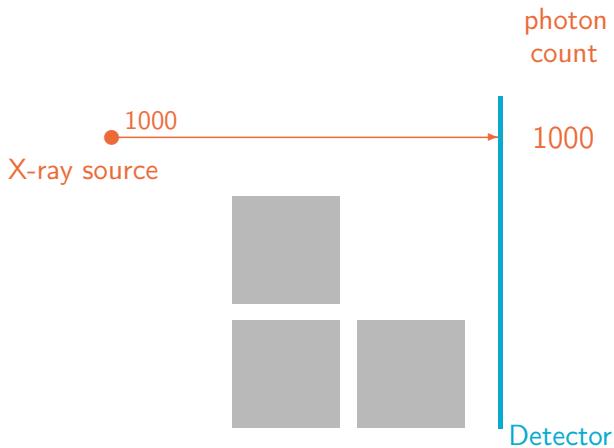
**X-ray intensity attenuates inside matter,  
here shown with a homogeneous block**

(Loading video)

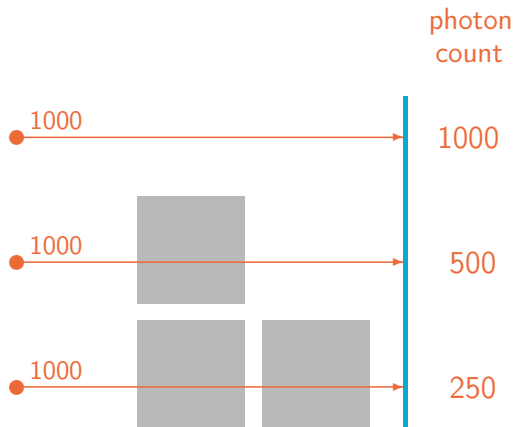
**X-ray intensity attenuates inside matter,  
here shown with two homogeneous blocks**

(Loading video)

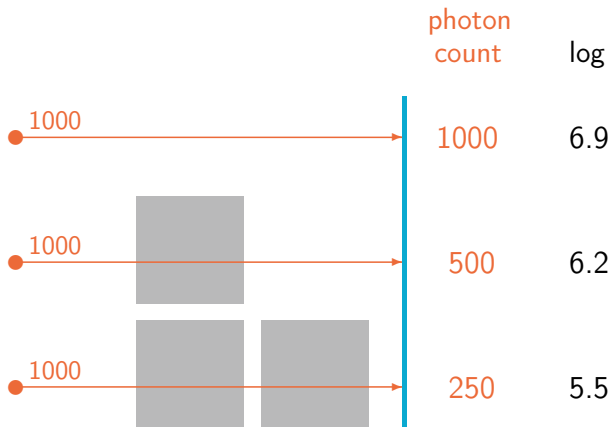
A digital X-ray detector counts how many photons arrive at each pixel



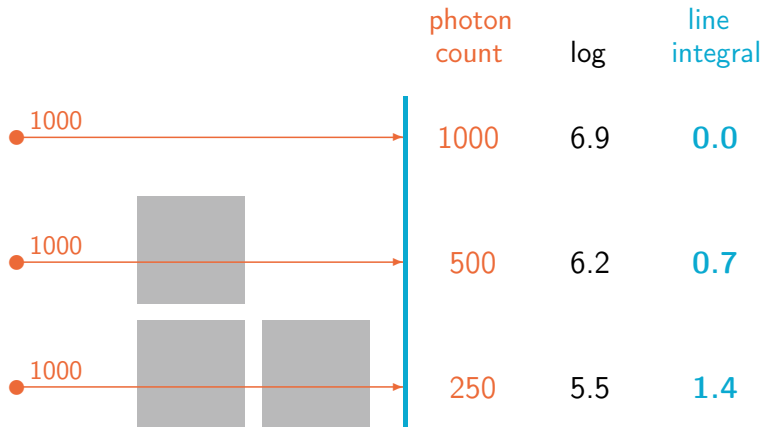
## Adding material between the source and detector reveals the exponential X-ray attenuation law



We take logarithm of the photon counts to compensate for the exponential attenuation law



Final calibration step is to subtract the logarithms from the empty space value (here 6.9)



**After calibration we are observing how much  
attenuating matter the X-ray encounters**

(Loading video)

**This sweeping movement is the data collection mode of first-generation CT scanners**

(Loading video)

Rotating around the object allows us to form the so-called *sinogram*

(Loading video)

**This is an illustration of the standard  
reconstruction by filtered back-projection**

(Loading video)

# Outline

Inverse problems and ill-posedness

## X-ray tomography

Mathematical model of X-ray attenuation

Tomographic imaging with sparse data

Regularized inversion

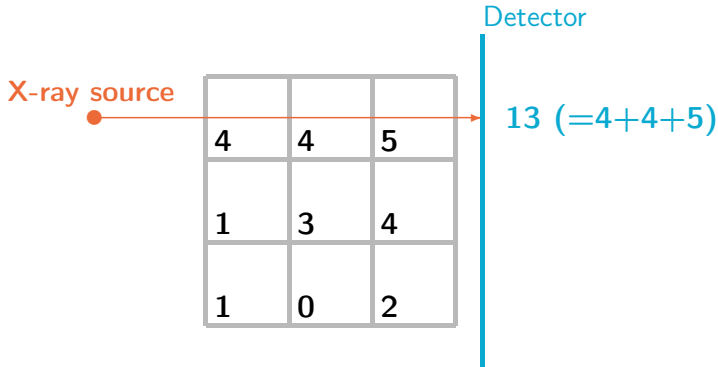
Industrial case study: low-dose 3D dental X-ray imaging

Conclusion: linear and nonlinear inverse problems

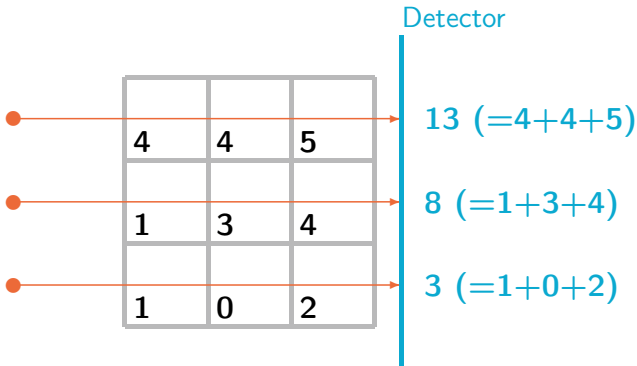
Let us study a simple two-dimensional example of tomographic imaging

4	4	5
1	3	4
1	0	2

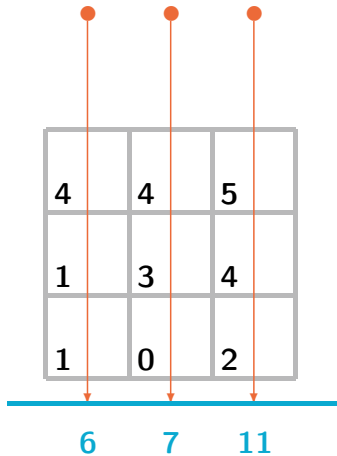
Tomography is based on measuring densities of matter using X-ray attenuation data



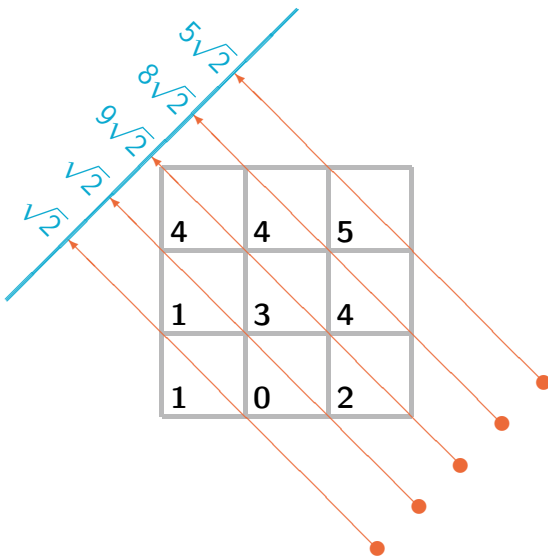
A projection image is produced by parallel X-rays and several detector pixels (here three pixels)



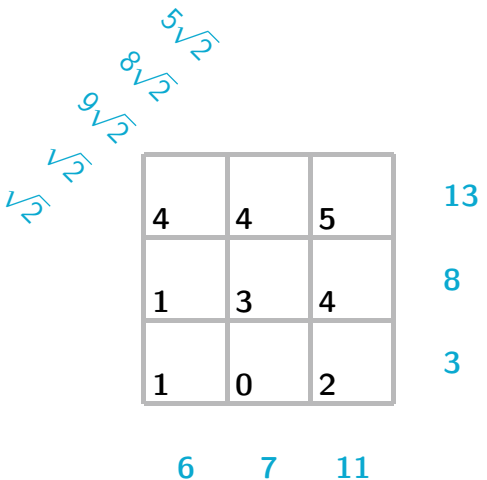
For tomographic imaging it is essential to record projection images from different directions



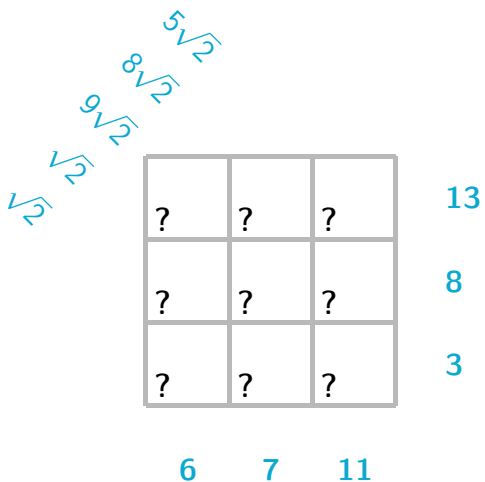
The length of X-rays traveling inside each pixel is important, thus here the square roots



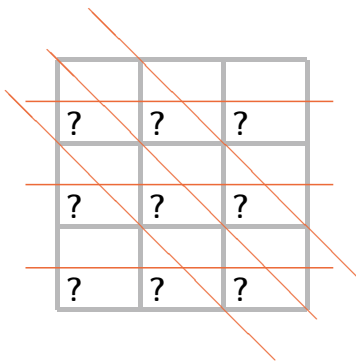
The direct problem of tomography is to find the projection images from known tissue



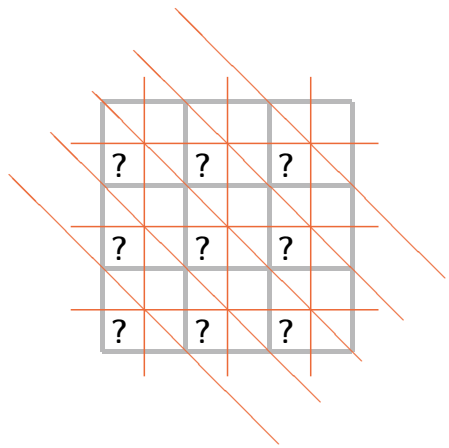
The inverse problem of tomography is to reconstruct the interior from X-ray data



# The limited-angle problem is harder than the full-angle problem

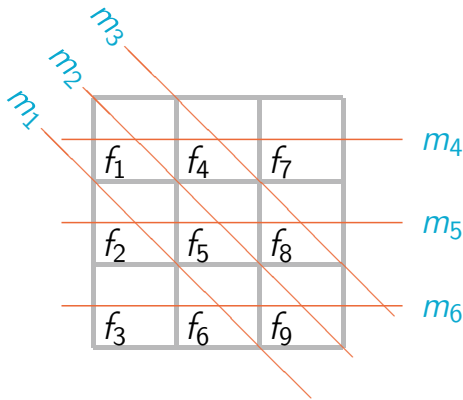


9 unknowns,  
6 equations



9 unknowns,  
11 equations

We write the reconstruction problem  
in matrix form

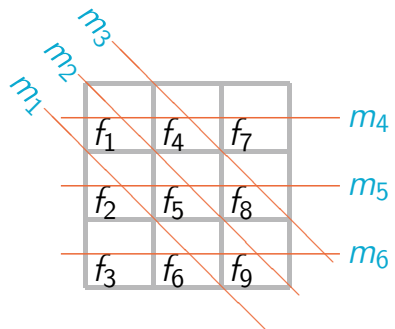


$$f = \begin{bmatrix} f_1 \\ f_2 \\ f_3 \\ f_4 \\ f_5 \\ f_6 \\ f_7 \\ f_8 \\ f_9 \end{bmatrix}, \quad m = \begin{bmatrix} m_1 \\ m_2 \\ m_3 \\ m_4 \\ m_5 \\ m_6 \end{bmatrix},$$

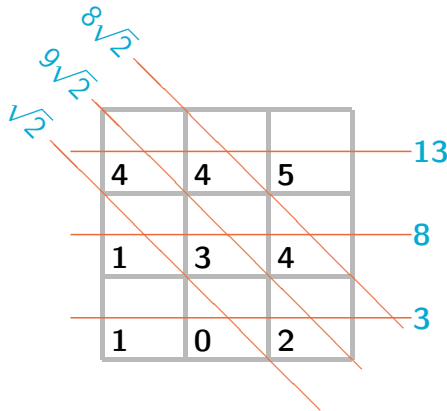
Measurement model:  $m = Af + \varepsilon$

This is the matrix equation related to the above measurement

$$\begin{bmatrix} m_1 \\ m_2 \\ m_3 \\ m_4 \\ m_5 \\ m_6 \end{bmatrix} = \begin{bmatrix} 0 & \sqrt{2} & 0 & 0 & 0 & \sqrt{2} & 0 & 0 & 0 \\ \sqrt{2} & 0 & 0 & 0 & \sqrt{2} & 0 & 0 & 0 & \sqrt{2} \\ 0 & 0 & 0 & \sqrt{2} & 0 & 0 & 0 & \sqrt{2} & 0 \\ 1 & 0 & 0 & 1 & 0 & 0 & 1 & 0 & 0 \\ 0 & 1 & 0 & 0 & 1 & 0 & 0 & 1 & 0 \\ 0 & 0 & 1 & 0 & 0 & 1 & 0 & 0 & 1 \end{bmatrix} \begin{bmatrix} f_1 \\ f_2 \\ f_3 \\ f_4 \\ f_5 \\ f_6 \\ f_7 \\ f_8 \\ f_9 \end{bmatrix} + \begin{bmatrix} \varepsilon_1 \\ \varepsilon_2 \\ \varepsilon_3 \\ \varepsilon_4 \\ \varepsilon_5 \\ \varepsilon_6 \end{bmatrix}$$



In limited-angle imaging, different objects may produce the same data

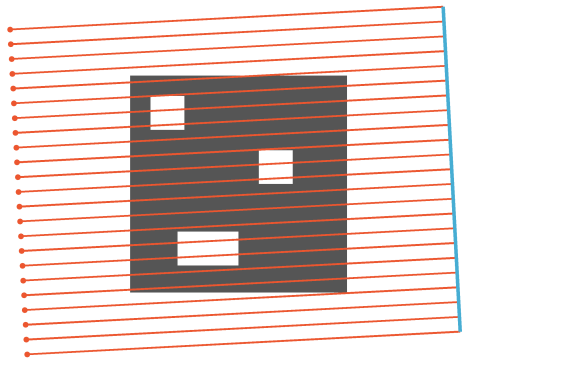


5	6	2
1	5	2
4	0	-1

9	1	3
1	0	7
3	0	0

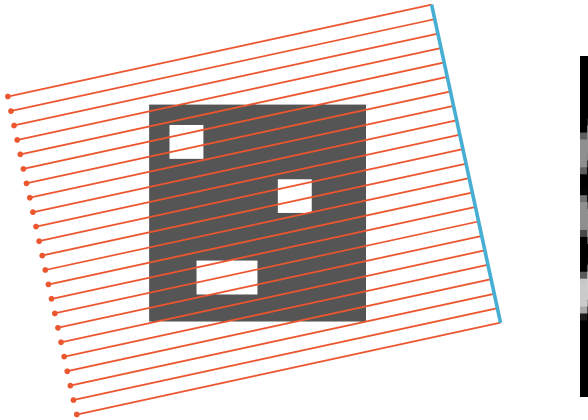
Mathematically this means that the matrix  $A$  has nontrivial kernel.

# Construction of the sinogram



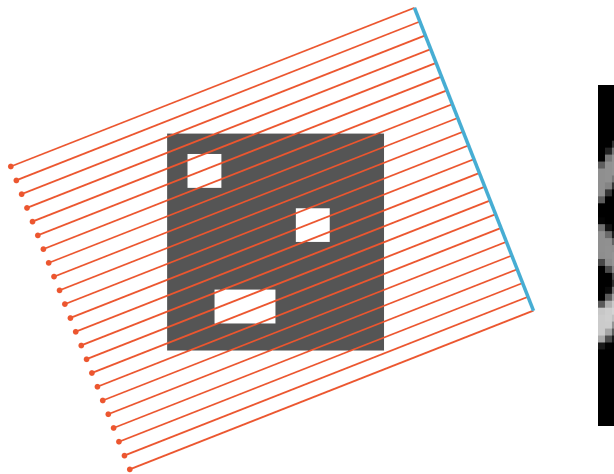
Angle of X-rays: 3.0 degrees

# Construction of the sinogram



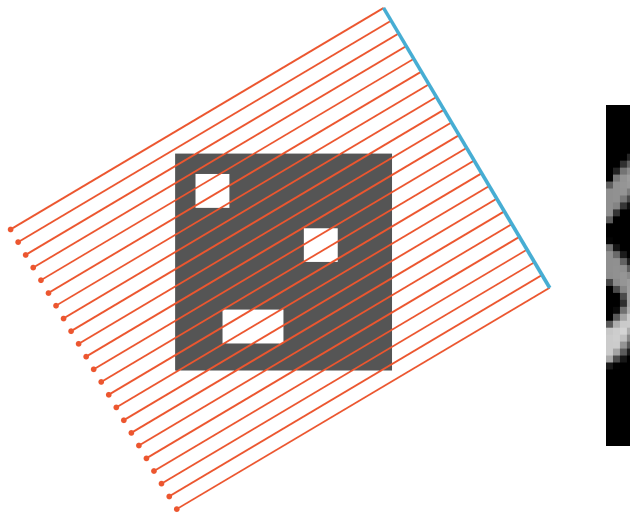
Angle of X-rays: 12.2 degrees

# Construction of the sinogram



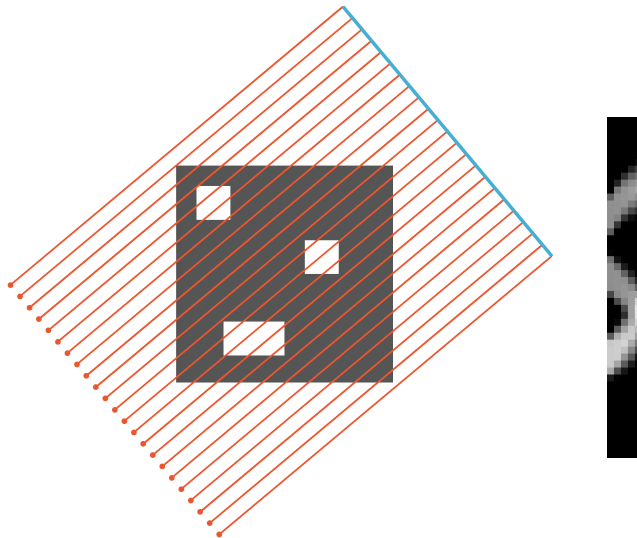
Angle of X-rays: 21.5 degrees

# Construction of the sinogram



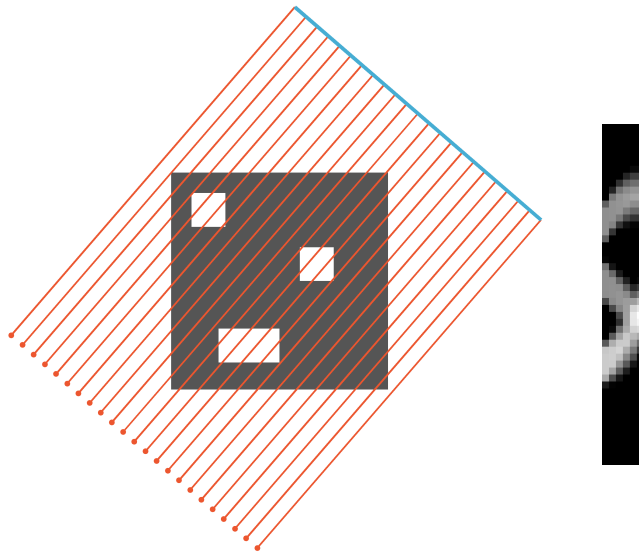
Angle of X-rays: 30.7 degrees

# Construction of the sinogram



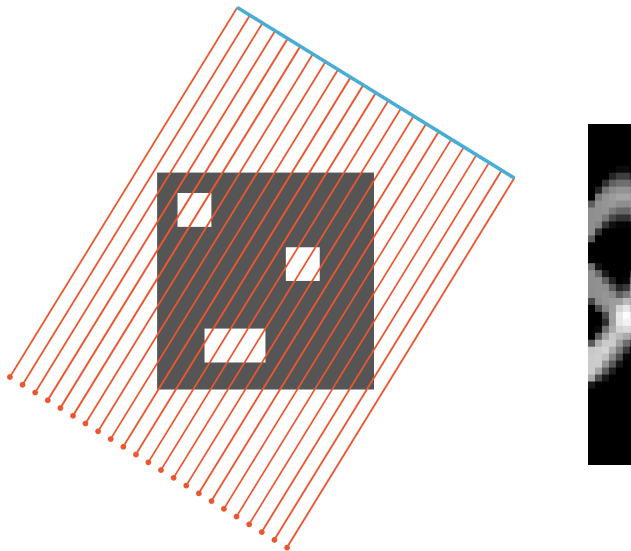
Angle of X-rays: 39.9 degrees

# Construction of the sinogram



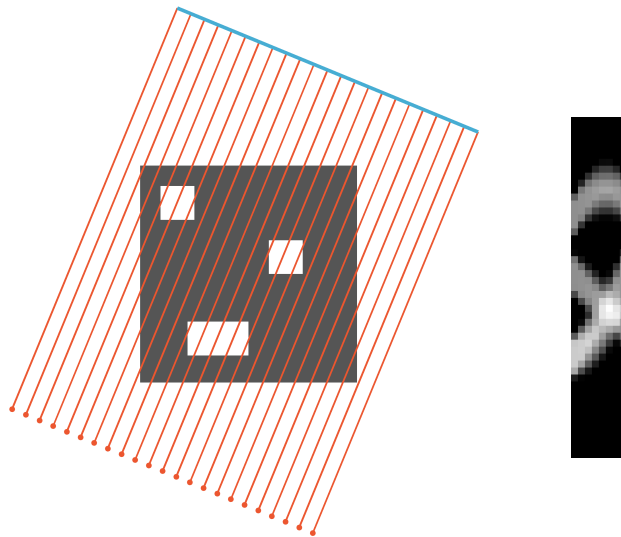
Angle of X-rays: 49.2 degrees

# Construction of the sinogram



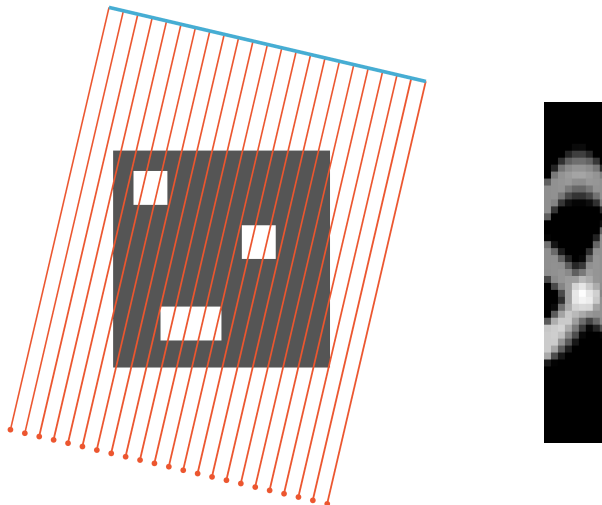
Angle of X-rays: 58.4 degrees

# Construction of the sinogram



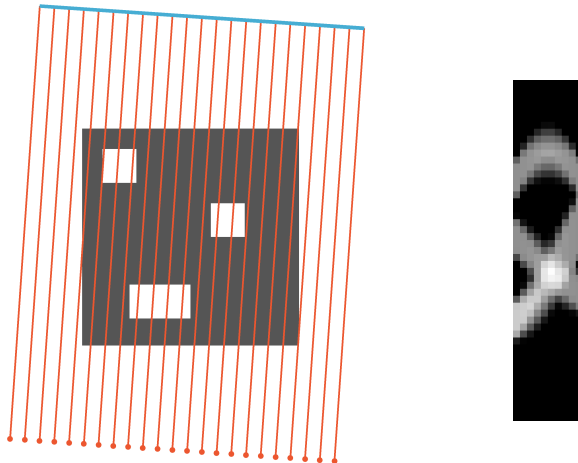
Angle of X-rays: 67.6 degrees

# Construction of the sinogram



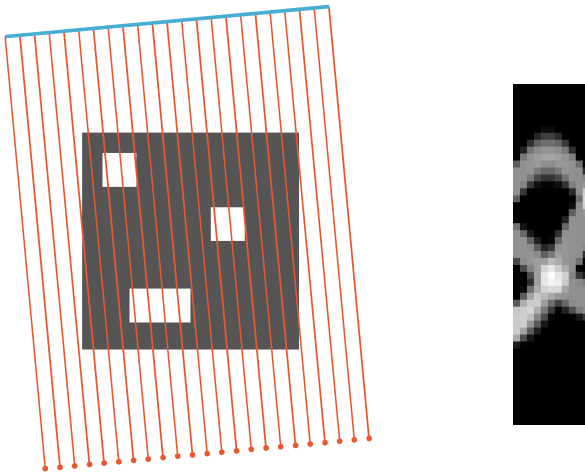
Angle of X-rays: 76.8 degrees

# Construction of the sinogram



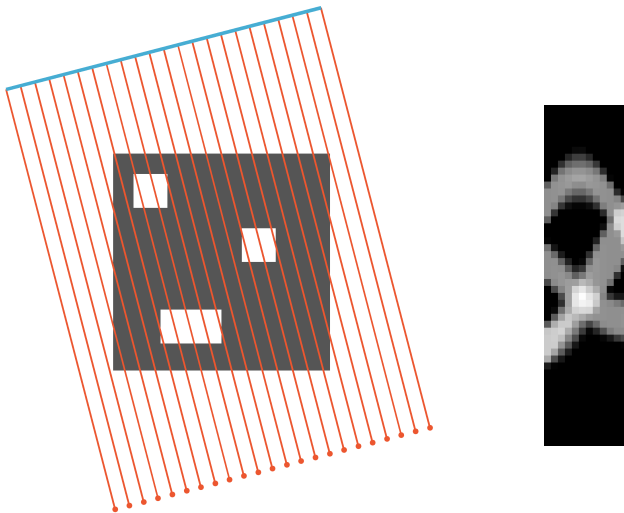
Angle of X-rays: 86.1 degrees

# Construction of the sinogram



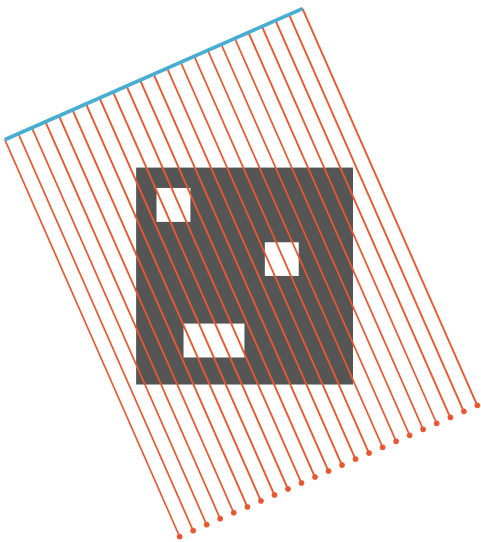
Angle of X-rays: 95.3 degrees

# Construction of the sinogram



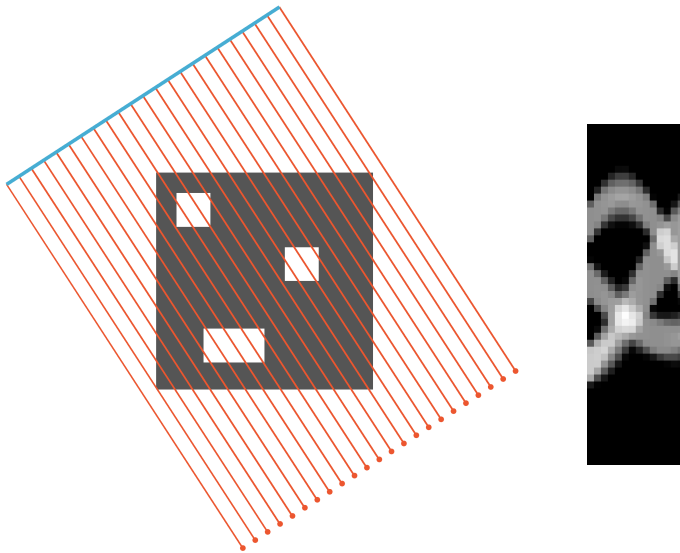
Angle of X-rays: 104.5 degrees

# Construction of the sinogram



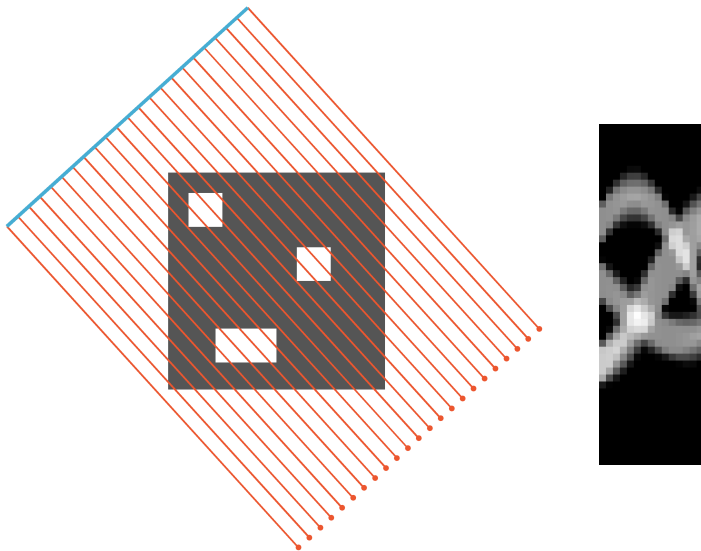
Angle of X-rays: 113.8 degrees

# Construction of the sinogram



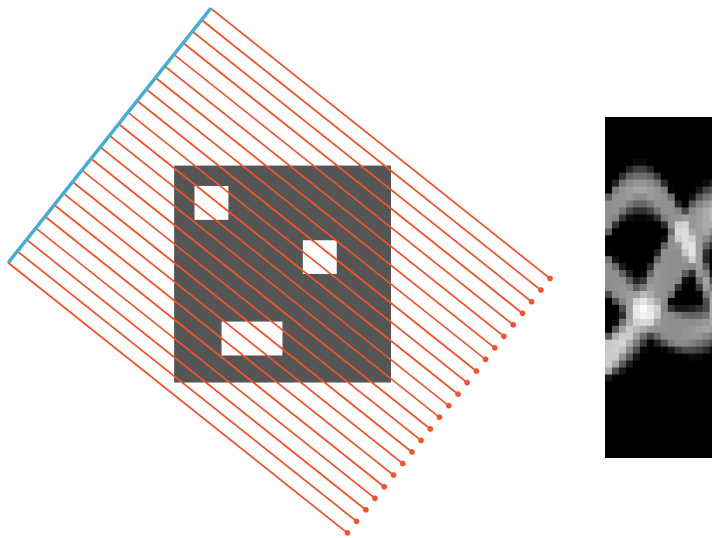
Angle of X-rays: 123.0 degrees

# Construction of the sinogram



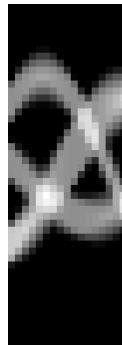
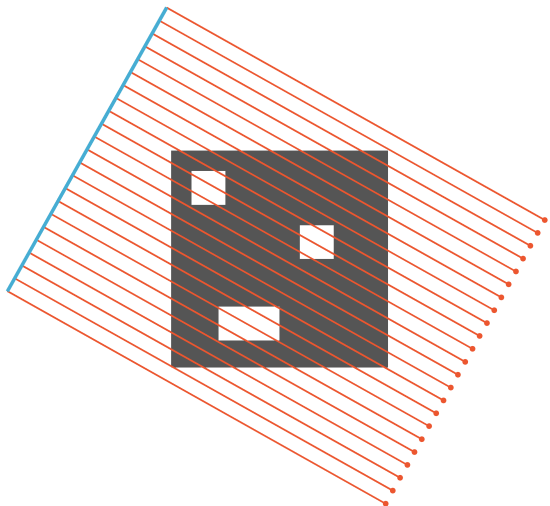
Angle of X-rays: 132.2 degrees

# Construction of the sinogram



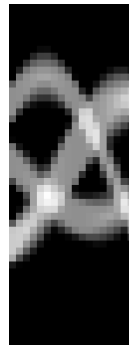
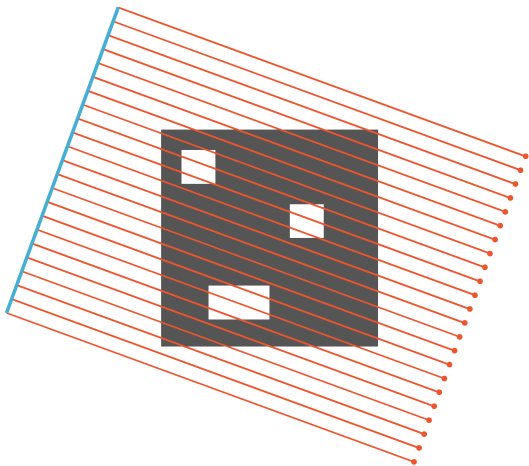
Angle of X-rays: 141.5 degrees

# Construction of the sinogram



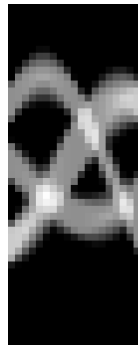
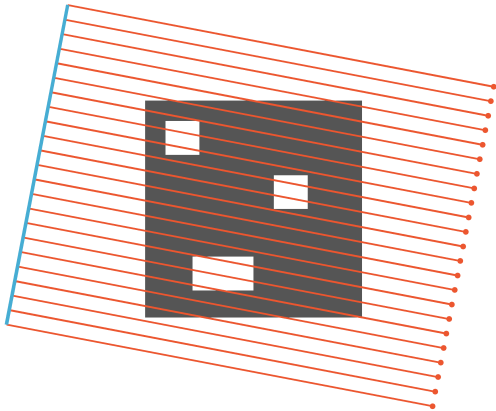
Angle of X-rays: 150.7 degrees

# Construction of the sinogram



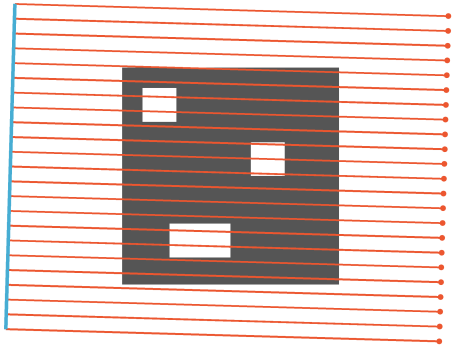
Angle of X-rays: 159.9 degrees

# Construction of the sinogram



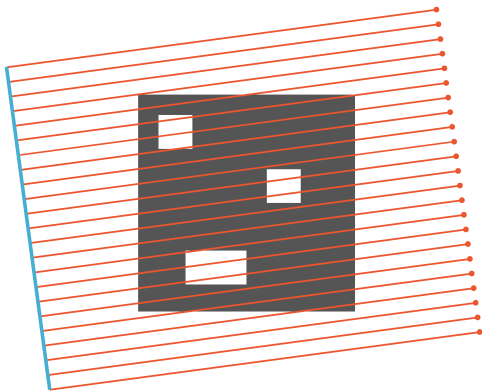
Angle of X-rays: 169.2 degrees

# Construction of the sinogram



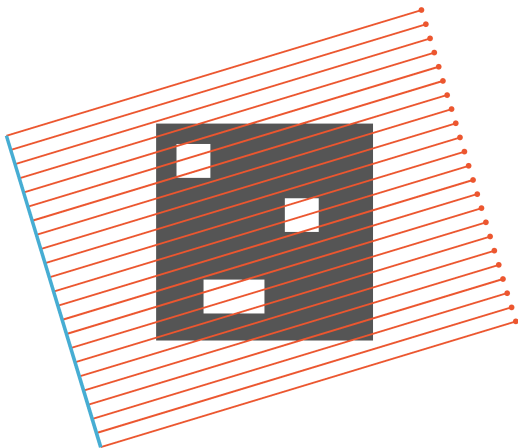
Angle of X-rays: 178.4 degrees

# Construction of the sinogram



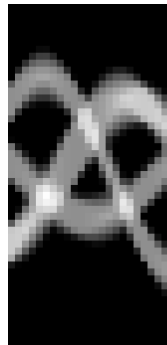
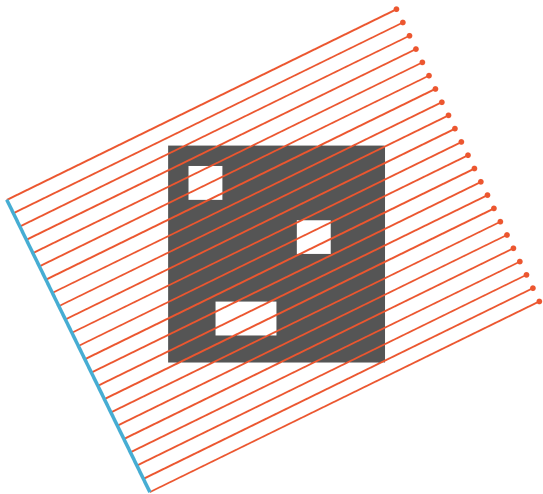
Angle of X-rays: 187.6 degrees

# Construction of the sinogram



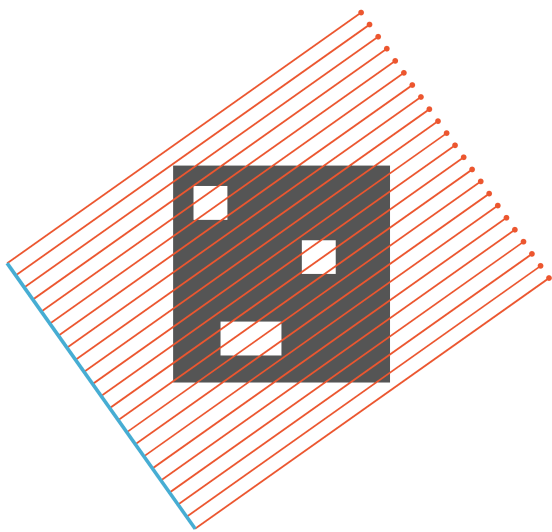
Angle of X-rays: 196.8 degrees

# Construction of the sinogram



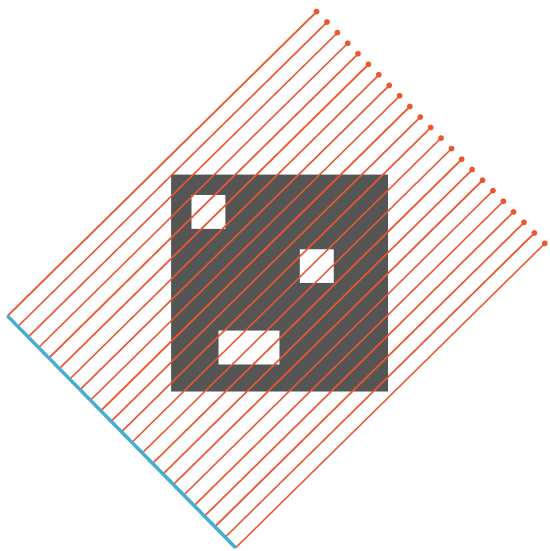
Angle of X-rays: 206.1 degrees

# Construction of the sinogram



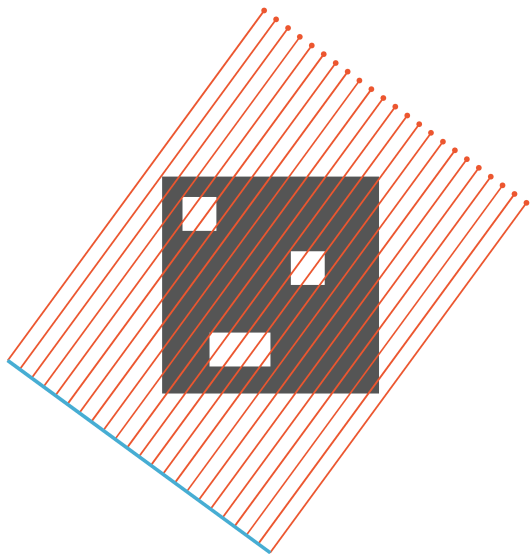
Angle of X-rays: 215.3 degrees

# Construction of the sinogram



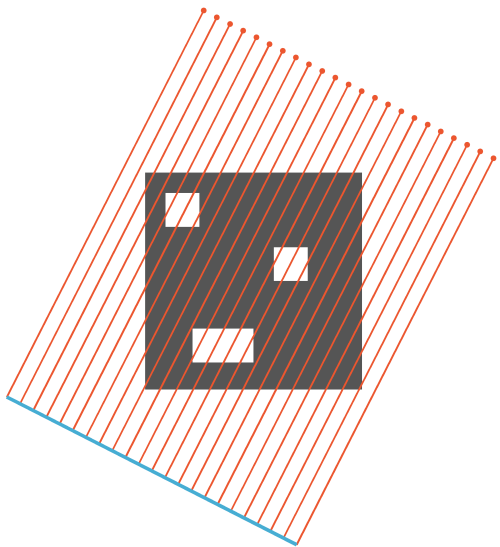
Angle of X-rays: 224.5 degrees

# Construction of the sinogram



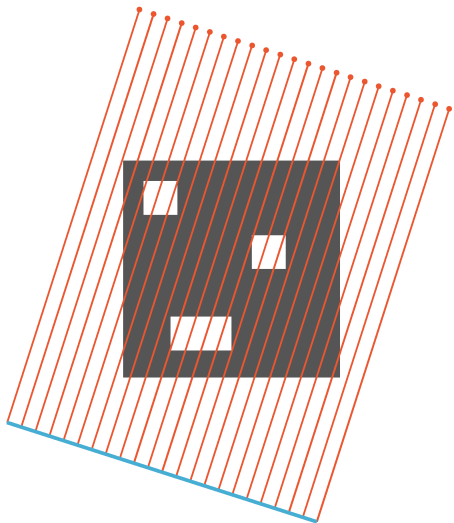
Angle of X-rays: 233.8 degrees

# Construction of the sinogram



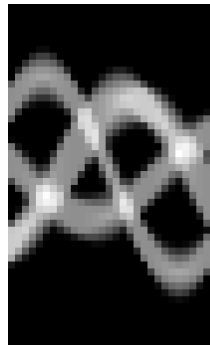
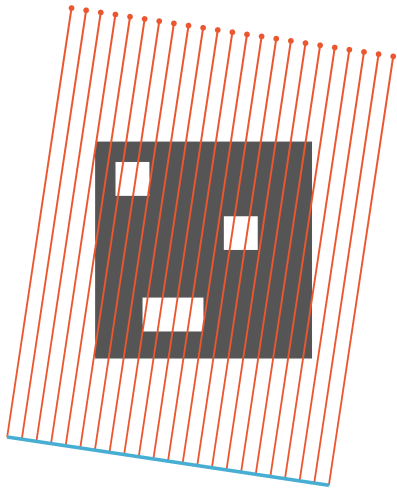
Angle of X-rays: 243.0 degrees

# Construction of the sinogram



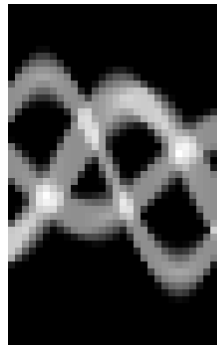
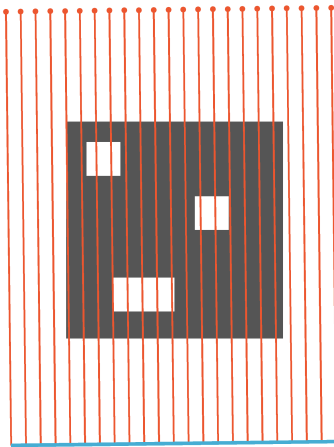
Angle of X-rays: 252.2 degrees

# Construction of the sinogram



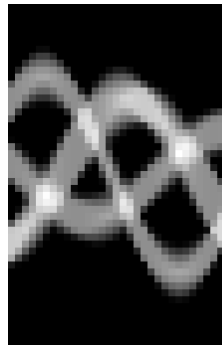
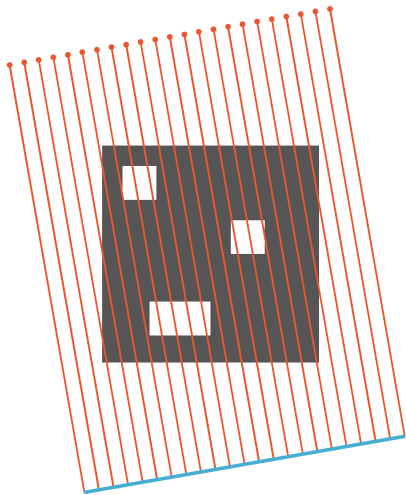
Angle of X-rays: 261.5 degrees

# Construction of the sinogram



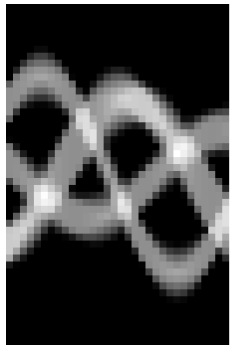
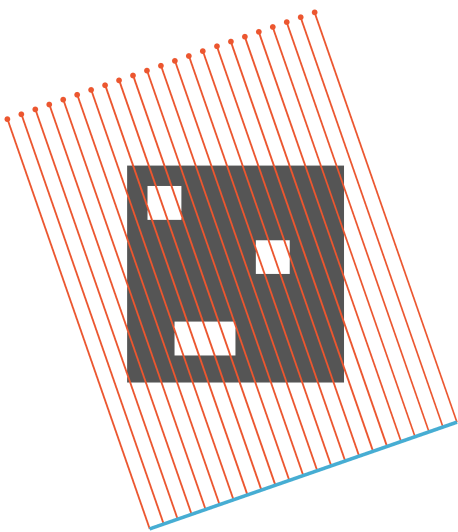
Angle of X-rays: 270.7 degrees

# Construction of the sinogram



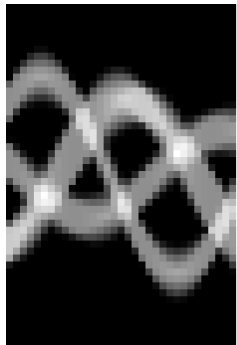
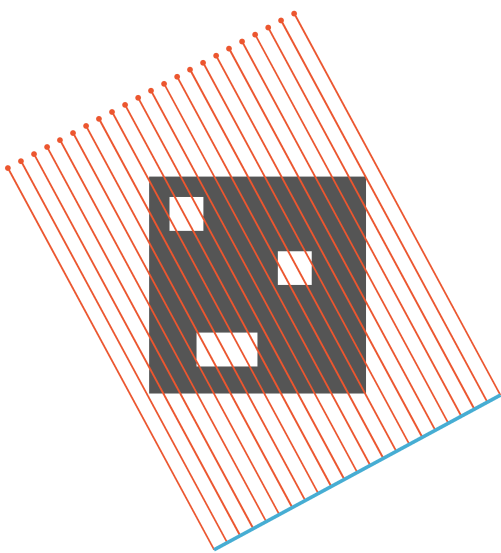
Angle of X-rays: 279.9 degrees

# Construction of the sinogram



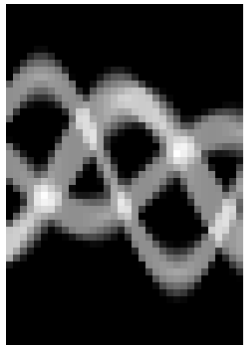
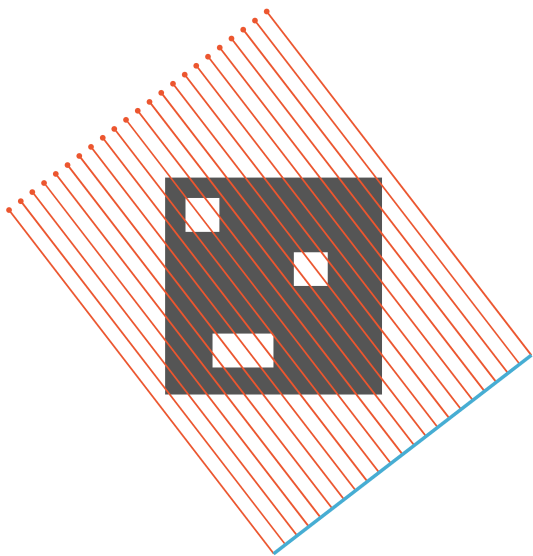
Angle of X-rays: 289.2 degrees

# Construction of the sinogram



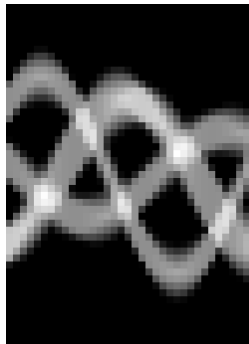
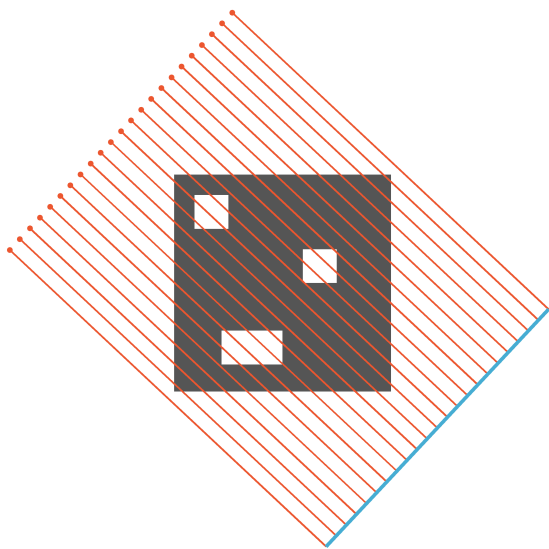
Angle of X-rays: 298.4 degrees

# Construction of the sinogram



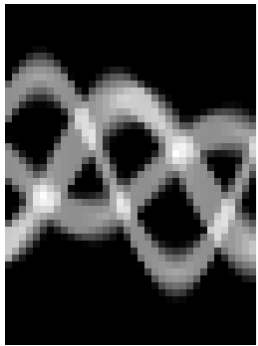
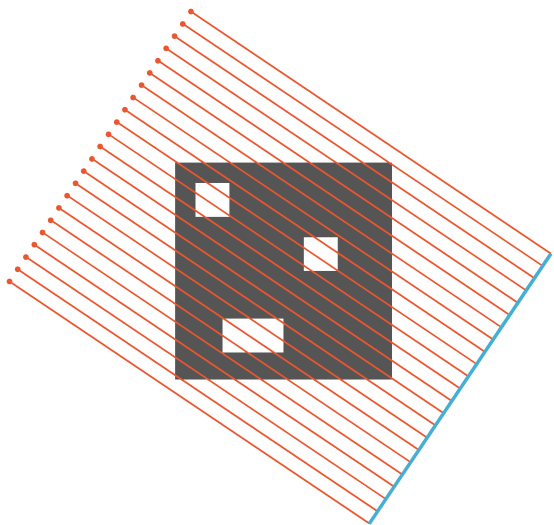
Angle of X-rays: 307.6 degrees

# Construction of the sinogram



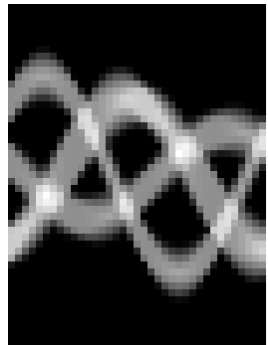
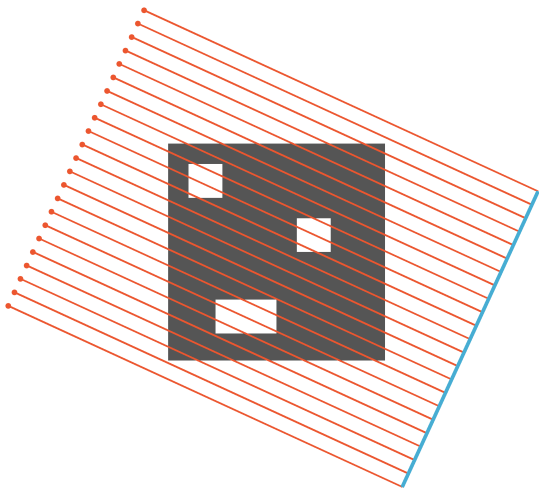
Angle of X-rays: 316.8 degrees

# Construction of the sinogram



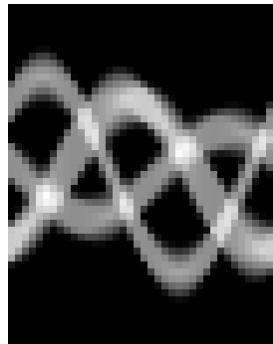
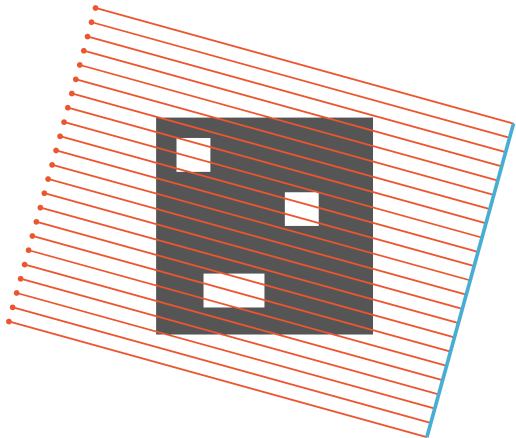
Angle of X-rays: 326.1 degrees

# Construction of the sinogram



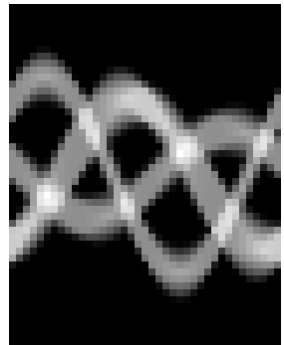
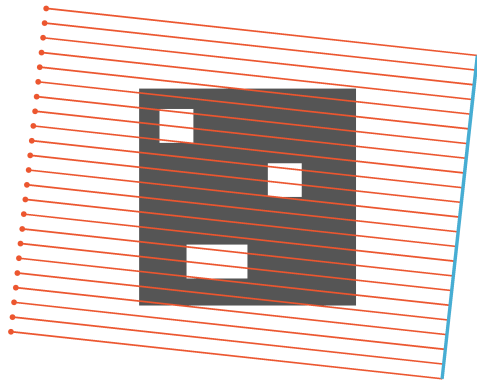
Angle of X-rays: 335.3 degrees

# Construction of the sinogram



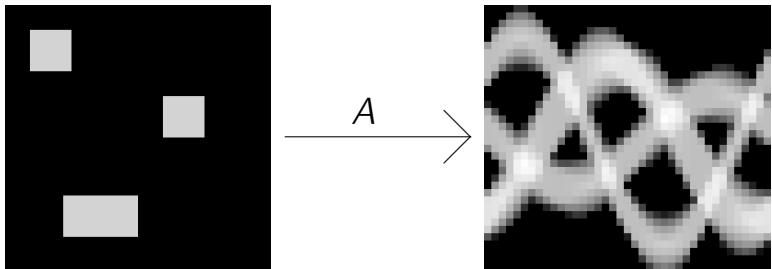
Angle of X-rays: 344.5 degrees

# Construction of the sinogram



Angle of X-rays: 353.8 degrees

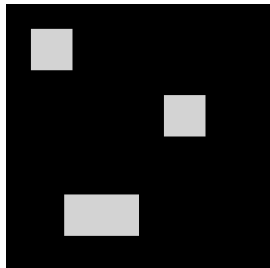
We have object and data for the inverse problem



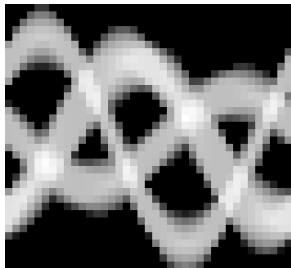
$$f \in \mathbb{R}^{32 \times 32}$$

$$Af \in \mathbb{R}^{49 \times 39}$$

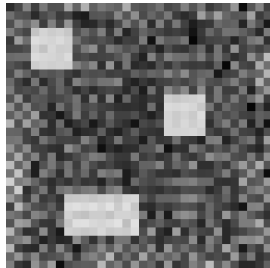
## Illustration of the ill-posedness of tomography



$$A \rightarrow$$



Difference 0.02672



$$A \rightarrow$$

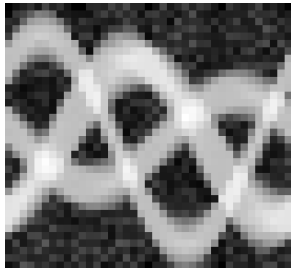
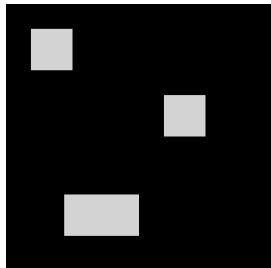
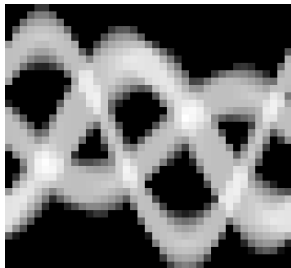


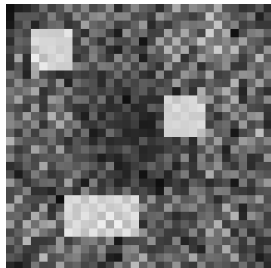
## Illustration of the ill-posedness of tomography



$$A \rightarrow$$



Difference 0.00899



$$A \rightarrow$$

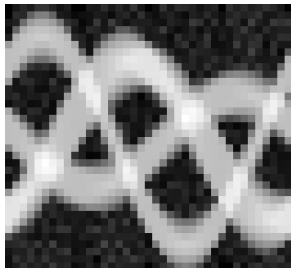
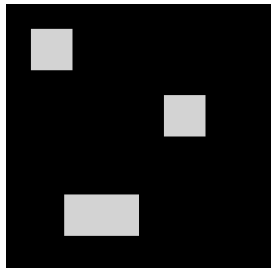


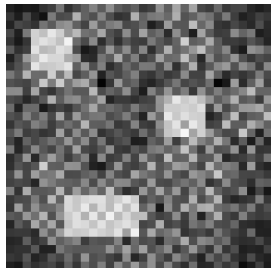
## Illustration of the ill-posedness of tomography



$$A \rightarrow$$



Difference 0.00254



$$A \rightarrow$$

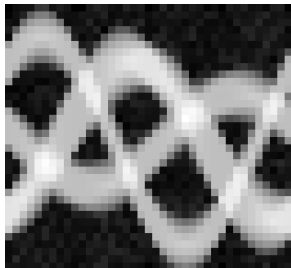
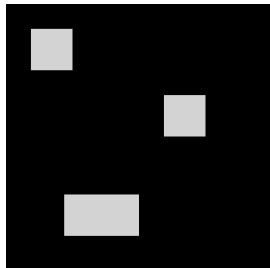
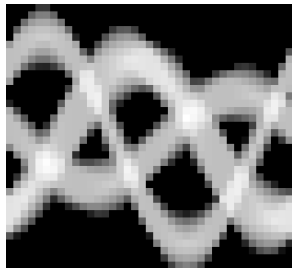


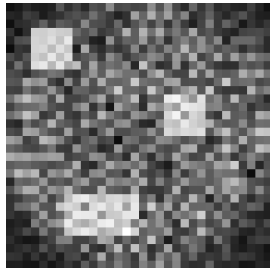
## Illustration of the ill-posedness of tomography



$$A \rightarrow$$



Difference 0.00124



$$A \rightarrow$$

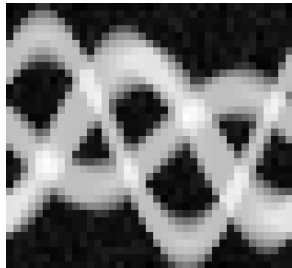
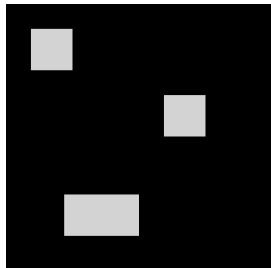
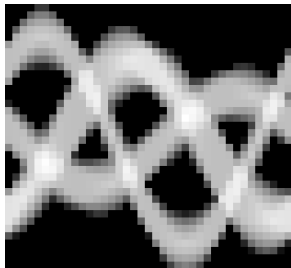


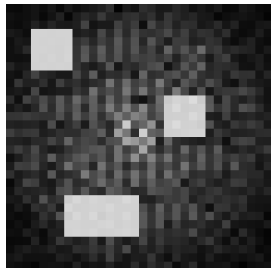
## Illustration of the ill-posedness of tomography



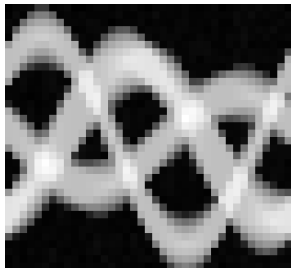
$$A \rightarrow$$



Difference 0.00004



$$A \rightarrow$$



# Outline

Inverse problems and ill-posedness

## X-ray tomography

Mathematical model of X-ray attenuation

Tomographic imaging with sparse data

### Regularized inversion

Industrial case study: low-dose 3D dental X-ray imaging

Conclusion: linear and nonlinear inverse problems

# Recall Hadamard's conditions for a well-posed problem



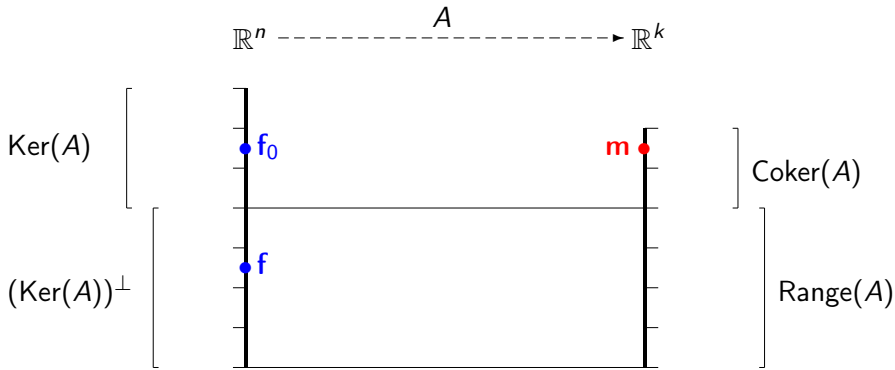
Hadamard (1903): a problem is well-posed if the following conditions hold.

1. A solution exists,
2. The solution is unique,
3. The solution depends continuously on the input.

III-posed inverse problem:

Input noisy data  $m = Af + \varepsilon$ , recover  $f$ .

## Hadamard's conditions in a linear inverse problem with forward map given by a matrix $A$



The matrix  $A$  maps bijectively between  $(\text{Ker}(A))^\perp$  and  $\text{Range}(A)$ . However, decreasing singular values may make this bijection unstable, leading to trouble with Hadamard's condition 3.

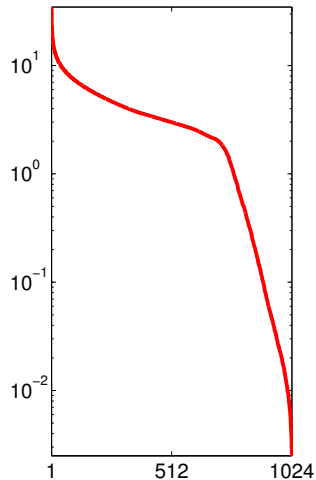
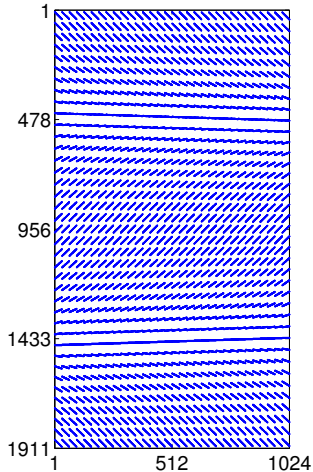
**Singular Value Decomposition for  $k \times n$  matrix  $A$ :**  
 $A = UDV^T$  with  $UU^T = I = U^T U$  and  $VV^T = I = V^T V$

$$A = UDV^T = U \begin{bmatrix} d_1 & 0 & \cdots & 0 & & \cdots & 0 \\ 0 & d_2 & & & & & \vdots \\ \vdots & & \ddots & & & & \\ & & & d_r & & & \\ & & & & 0 & & \\ \vdots & & & & & \ddots & \vdots \\ 0 & \cdots & & & & \cdots & 0 \end{bmatrix} V^T$$

The singular values  $d_j$  satisfy  $d_1 \geq d_2 \geq \cdots \geq d_r > 0$   
 and  $d_{r+1} = d_{r+2} = \cdots = d_{\min\{k,n\}} = 0$ . Note that  $r = \text{rank}(A)$ .

If  $n = k$  and all singular values are positive, then  $A$  is invertible.  
 However, the *condition number*  $\text{cond}(A) := d_1/d_r$  may be large.  
 In that case  $A^{-1}$  is a numerically unstable matrix.

# Singular Value Decomposition (SVD) of the above tomographic measurement matrix $A$

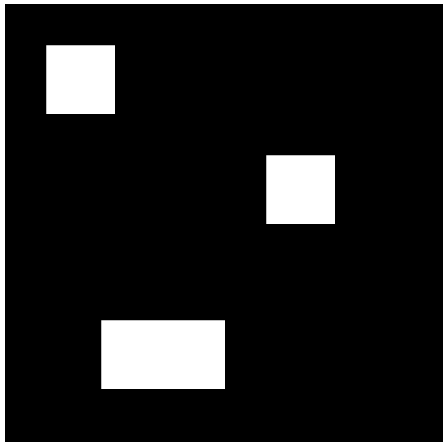


The Moore-Penrose pseudoinverse takes care of Hadamard's conditions 1 and 2

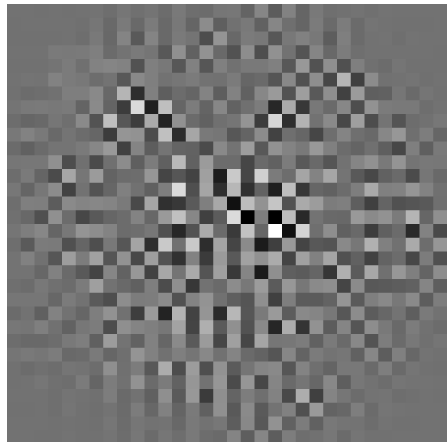
$$A^\dagger = V D^\dagger U^T = V \begin{bmatrix} 1/d_1 & 0 & \cdots & 0 & \cdots & 0 \\ 0 & 1/d_2 & & & & \vdots \\ \vdots & & \ddots & & & \\ & & & 1/d_r & & 0 \\ & & & & & \ddots \\ \vdots & & & & & \vdots \\ 0 & \cdots & & & \cdots & 0 \end{bmatrix} U^T$$

We can compute **naive reconstruction** as the uniquely defined *minimum norm solution*  $x^\dagger := A^\dagger m$ .

# Naive reconstruction using the Moore-Penrose pseudoinverse; data has 0.1% relative noise



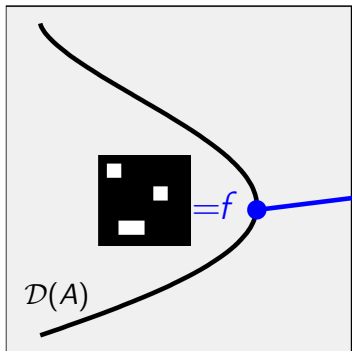
Original phantom, values between zero (black) and one (white)



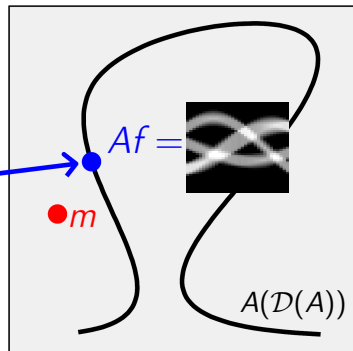
Naive reconstruction with minimum -14.9 and maximum 18.5

# Inverse problem of X-ray tomography: given noisy sinogram, find a stable approximation to $f$

Model space  $X = \mathbb{R}^{32 \times 32}$

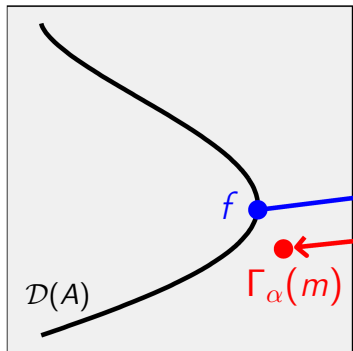


Data space  $Y = \mathbb{R}^{32 \times 49}$

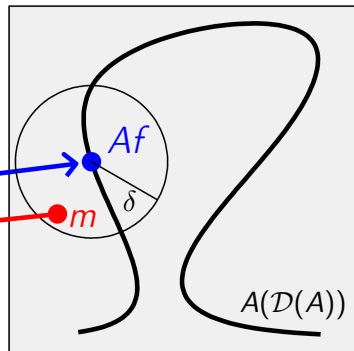


# Robust solution of ill-posed inverse problems requires regularization

Model space  $X = \mathbb{R}^{32 \times 32}$



Data space  $Y = \mathbb{R}^{39 \times 49}$



We need to define a family of continuous functions  $\Gamma_\alpha : Y \rightarrow X$  so that the reconstruction error  $\|\Gamma_{\alpha(\delta)}(m) - x\|_X$  vanishes asymptotically at the zero-noise level  $\delta \rightarrow 0$ .

# Tikhonov regularization is the classical method for noise-robust tomographic reconstruction

Write a penalty functional

$$\Phi(f) = \|Af - m\|_2^2 + \alpha\|f\|_2^2,$$

where  $0 < \alpha < \infty$  is a regularization parameter. Define  $\Gamma_\alpha(m)$  by

$$\Phi(\Gamma_\alpha(m)) = \min_{f \in X} \{\Phi(f)\}.$$

We denote

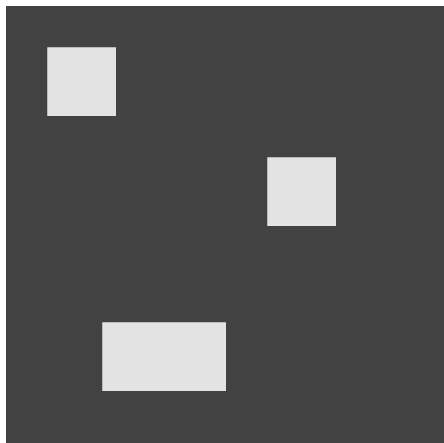
$$\Gamma_\alpha(m) = \arg \min_{f \in X} \{\|Af - m\|_2^2 + \alpha\|f\|_2^2\}.$$

Tikhonov regularization can be expressed as filtering the singular values of the matrix  $A$

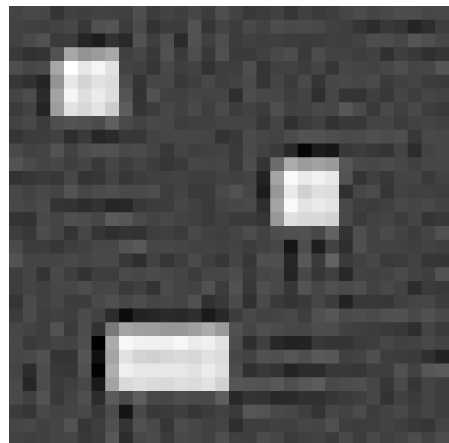
$$\Gamma_\alpha(\textcolor{red}{m}) = V \begin{bmatrix} \frac{d_1}{d_1^2 + \alpha} & 0 & \dots & 0 \\ 0 & \ddots & & \vdots \\ \vdots & & \ddots & 0 \\ 0 & \dots & 0 & \frac{d_{\min\{k,n\}}}{d_{\min\{k,n\}}^2 + \alpha} \end{bmatrix} U^T \textcolor{red}{m}$$

# Standard Tikhonov regularization

$$\arg \min_{f \in \mathbb{R}^n} \left\{ \|Af - m\|_2^2 + \alpha \|f\|_2^2 \right\}$$



Original phantom

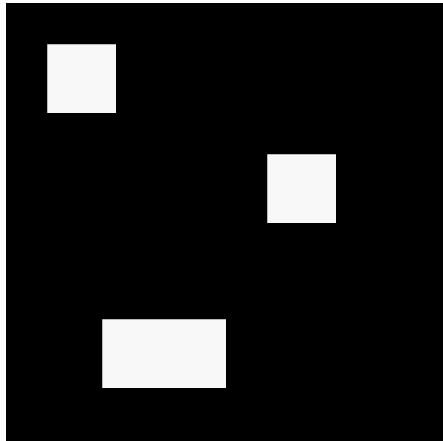


Reconstruction

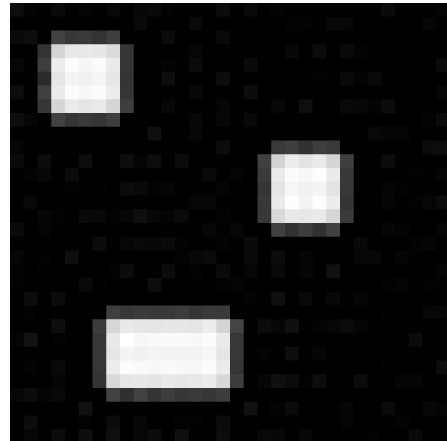
Relative square norm error 35%

# Constrained Tikhonov regularization

$$\arg \min_{f \in \mathbb{R}_+^n} \left\{ \|Af - m\|_2^2 + \alpha \|f\|_2^2 \right\}$$



Original phantom



Reconstruction

Relative square norm error 13%

## Recall the $L^p$ norms for $\mathbb{R}^n$

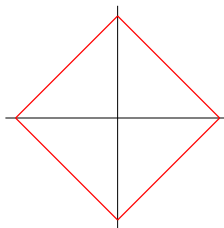
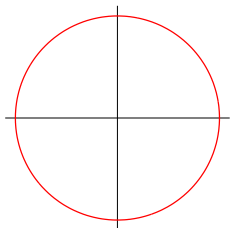
Let  $f \in \mathbb{R}^n$ . The  $L^p$  norms for  $1 \leq p < \infty$  are defined by

$$\|f\|_p = \left( \sum_{j=1}^n |f_j|^p \right)^{1/p}.$$

In particular we use the following two cases:

$$\|f\|_2^2 = \sum_{j=1}^n |f_j|^2,$$

$$\|f\|_1 = \sum_{j=1}^n |f_j|.$$



## Total variation (TV) regularization is a technique for preserving edges in the reconstruction

We consider calculating the minimizer of the TV functional

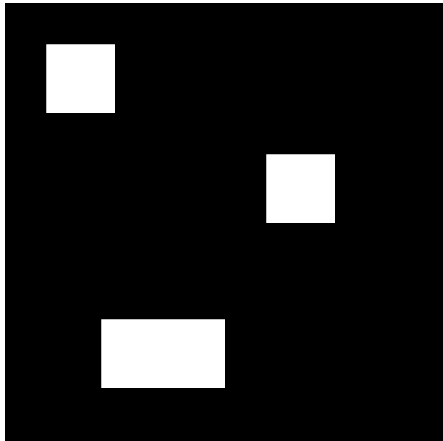
$$\begin{aligned} & \|Af - m\|_2^2 + \alpha \{\|L_H f\|_1 + \|L_V f\|_1\} \\ = & \|Af - m\|_2^2 + \alpha \left\{ \sum_j \sum_i \left( |f_{i(j+1)} - f_{ij}| + |f_{(i+1)j} - f_{ij}| \right) \right\} \end{aligned}$$

where  $L_H$  and  $L_V$  are horizontal and vertical first-order difference matrices. [Rudin, Osher and Fatemi 1992]

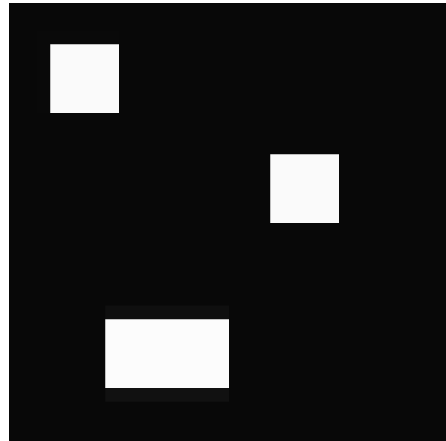
In very large-scale computations we approximate the absolute value function by  $|t|_\beta := \sqrt{t^2 + \beta}$ . Then we can use gradient-based minimization algorithms such as the Barzilai-Borwein method.

## Constrained TV regularization

$$\arg \min_{f \in \mathbb{R}_+^n} \left\{ \|Af - m\|_2^2 + \alpha \|\nabla f\|_1 \right\}$$



Original phantom



TV regularized reconstruction  
Relative square norm error 3%

In variational regularization, the penalty term expresses *a priori* knowledge about the unknown

Standard Tikhonov regularization:

$$\arg \min_{f \in \mathbb{R}^n} \left\{ \|Af - m\|_2^2 + \alpha \|f\|_2^2 \right\}$$

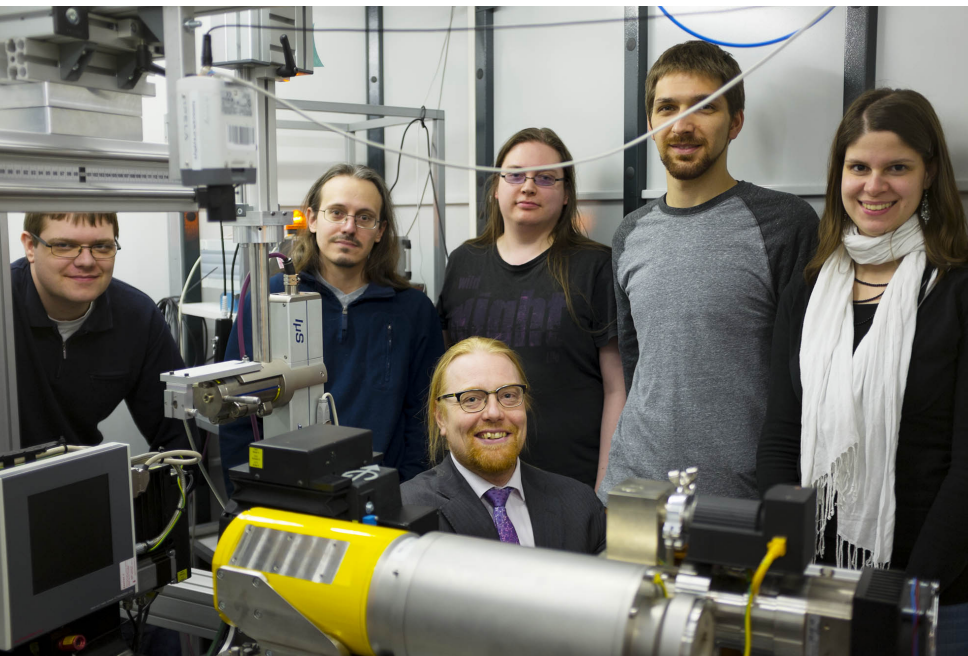
Non-negativity constrained Tikhonov regularization:

$$\arg \min_{f \in \mathbb{R}_+^n} \left\{ \|Af - m\|_2^2 + \alpha \|f\|_2^2 \right\}$$

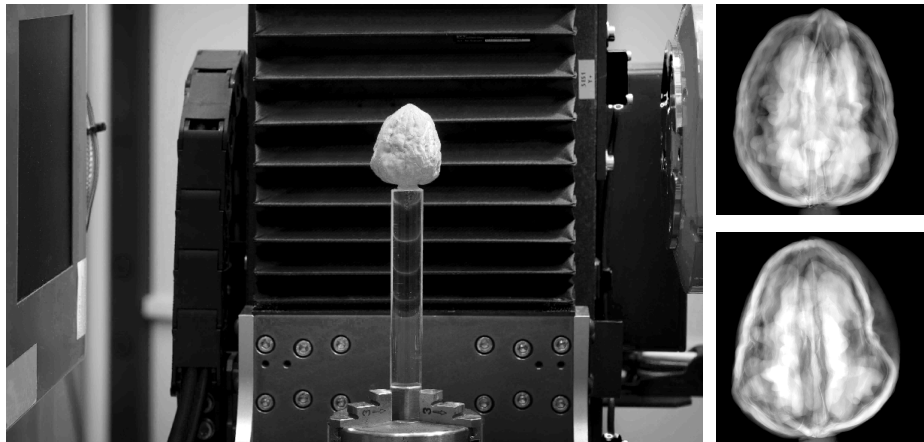
Non-negativity constrained Total Variation (TV) regularization:

$$\arg \min_{f \in \mathbb{R}_+^n} \left\{ \|Af - m\|_2^2 + \alpha \|\nabla f\|_1 \right\}$$

# This is Professor Keijo Hämäläinen's X-ray lab



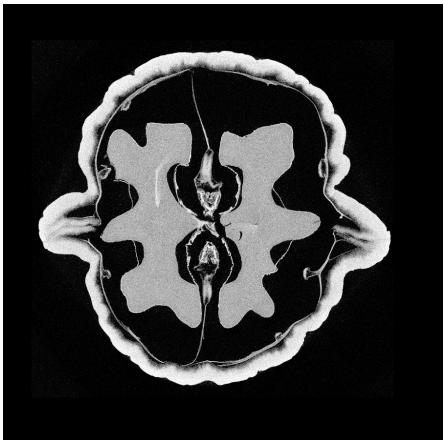
We collected X-ray projection data of a walnut from 1200 directions



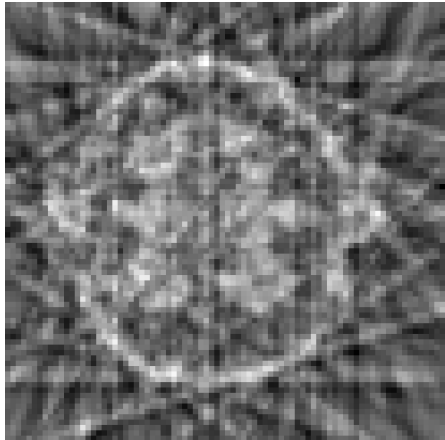
Laboratory and data collection by  
Keijo Hämäläinen and Aki Kallonen,  
University of Helsinki.

The data is openly available at  
<http://fips.fi/dataset.php>, thanks to  
Esa Niemi and Antti Kujanpää

# Reconstructions of a 2D slice through the walnut using filtered back-projection (FBP)

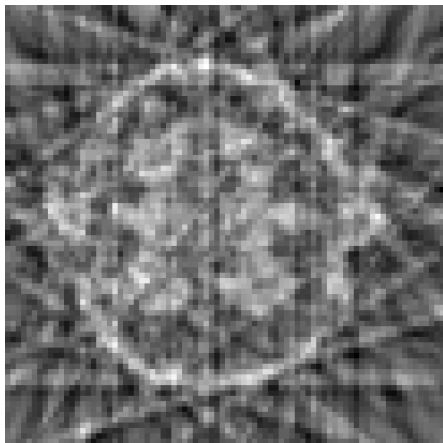


FBP with comprehensive data  
(1200 projections)

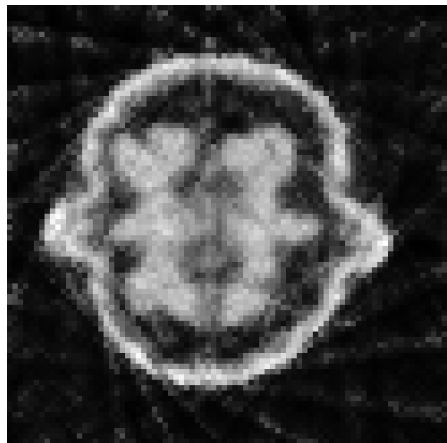


FBP with sparse data  
(20 projections)

# Sparse-data reconstruction of the walnut using non-negative Tikhonov regularization



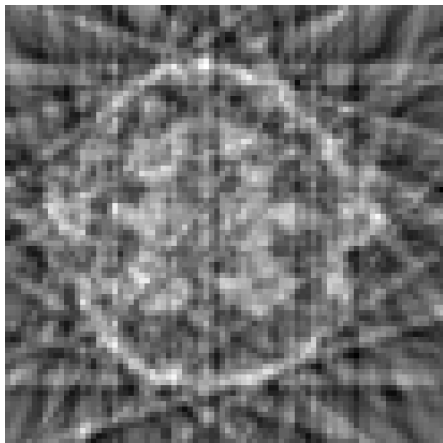
Filtered back-projection



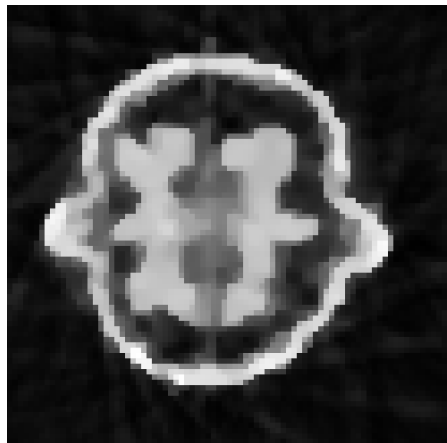
Constrained Tikhonov regularization

$$\arg \min_{f \in \mathbb{R}_+^n} \left\{ \|Af - m\|_2^2 + \alpha \|f\|_2^2 \right\}$$

# Sparse-data reconstruction of the walnut using non-negative Total Variation regularization



Filtered back-projection



Constrained TV regularization

$$\arg \min_{f \in \mathbb{R}_+^n} \left\{ \|Af - m\|_2^2 + \alpha \|\nabla f\|_1 \right\}$$

$$\text{TV tomography: } \arg \min_{f \in \mathbb{R}^n} \{ \|Af - m\|_2^2 + \alpha \|\nabla f\|_1 \}$$

- 1992 Rudin, Osher & Fatemi: denoise images by taking  $A = I$
- 1998 Delaney & Bresler
- 2001 Persson, Bone & Elmqvist
- 2003 Kolehmainen, S, Järvenpää, Kaipio, Koistinen, Lassas, Pirttilä & Somersalo (first TV work with measured X-ray data)
- 2006 Kolehmainen, Vanne, S, Järvenpää, Kaipio, Lassas & Kalke
- 2006 Sidky, Kao & Pan
- 2008 Liao & Sapiro
- 2008 Sidky & Pan
- 2008 Herman & Davidi
- 2009 Tang, Nett & Chen
- 2009 Duan, Zhang, Xing, Chen & Cheng
- 2010 Bian, Han, Sidky, Cao, Lu, Zhou & Pan
- 2011 Jensen, Jørgensen, Hansen & Jensen
- 2011 Tian, Jia, Yuan, Pan & Jiang
- 2012–present: dozens of articles indicated by Google Scholar

# Outline

Inverse problems and ill-posedness

## X-ray tomography

Mathematical model of X-ray attenuation

Tomographic imaging with sparse data

Regularized inversion

Industrial case study: low-dose 3D dental X-ray imaging

Conclusion: linear and nonlinear inverse problems

# The VT device was developed in 2001–2012 by

Nuutti Hyvönen

Seppo Järvenpää

Jari Kaipio

Martti Kalke

Petri Koistinen

Ville Kolehmainen

Matti Lassas

Jan Moberg

Kati Niinimäki

Juha Pirttilä

Maaria Rantala

Eero Saksman

Henri Setälä

Erkki Somersalo

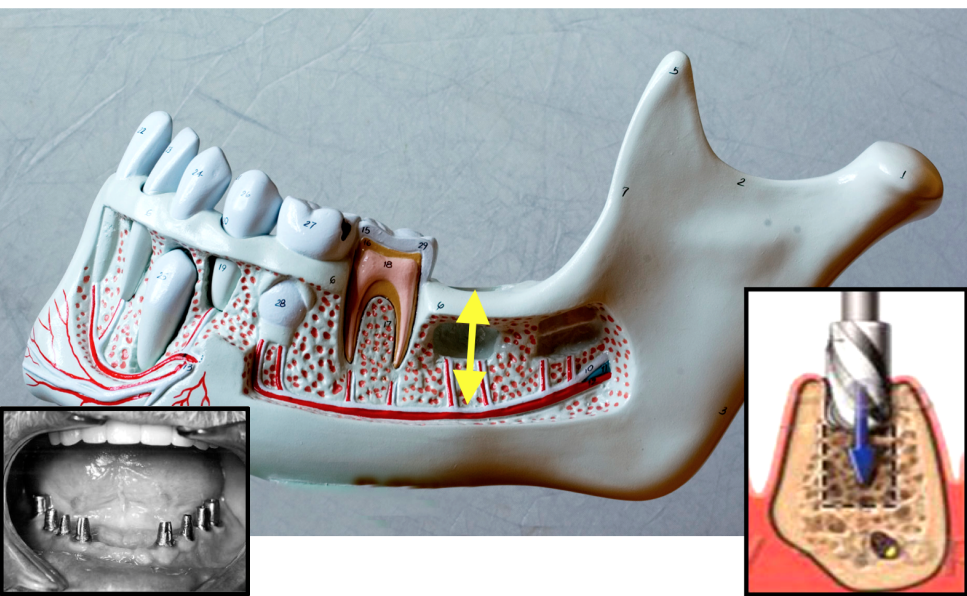
Antti Vanne

Simopekka Vänskä

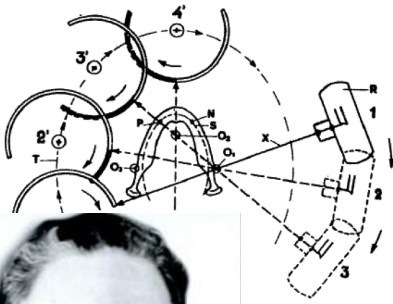
Richard L. Webber



# Application: dental implant planning, where a missing tooth is replaced with an implant



# Panoramic dental imaging shows all the teeth simultaneously



Panoramic imaging was invented by Yrjö Veli Paatero in the 1950's.



# Nowadays, a digital panoramic imaging device is standard equipment at dental clinics



A panoramic dental image offers a general overview showing all teeth and other dento-maxillofacial structures simultaneously.

Panoramic images are not suitable for dental implant planning because of unavoidable geometric distortion.

We reprogram the panoramic X-ray device so that it collects projection data by scanning

(Loading video)

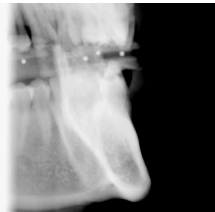
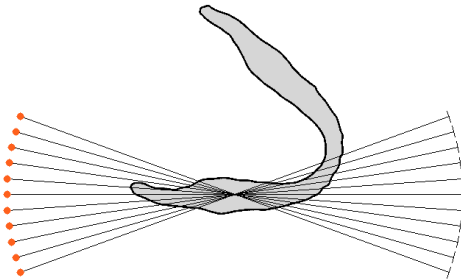
We reprogram the panoramic X-ray device so that it collects projection data by scanning

Number of projection images: 11

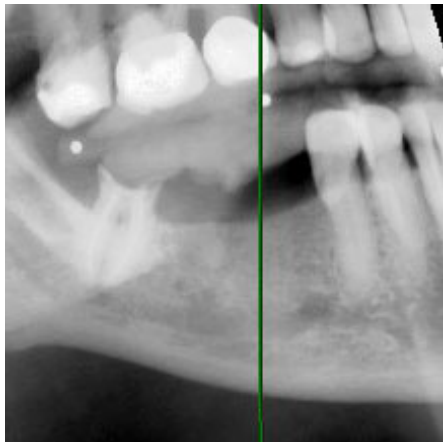
Angle of view: 40 degrees

Image size:  $1000 \times 1000$  pixels

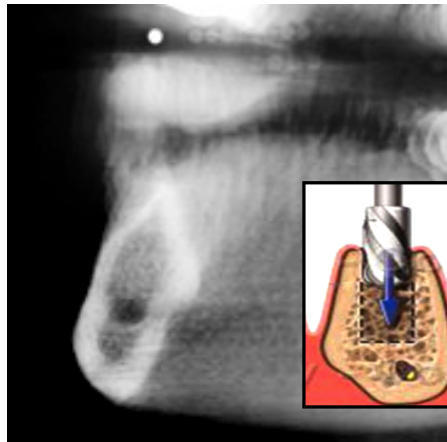
The unknown vector  $f$  has 7 000 000 elements.



Here are example images of an actual patient:  
navigation image (left) and desired slice (right).



Kolehmainen, Vanne, S, Järvenpää, Kaipio, Lassas & Kalke 2006,  
Kolehmainen, Lassas & S 2008



Cederlund, Kalke & Welander 2009,  
Hyvönen, Kalke, Lassas, Setälä & S  
2010, U.S. patent 7269241

# The radiation dose of the VT device is lowest among 3D dental imaging modalities

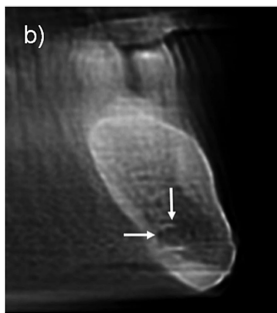
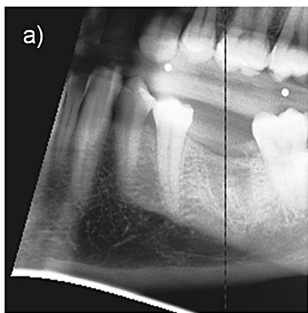
Modality	$\mu\text{Sv}$
Head CT	2100
CB Mercuray	558
i-Cat	193
NewTom 3G	59
<b>VT device</b>	<b>13</b>

[Ludlow, Davies-Ludlow, Brooks & Howerton 2006]

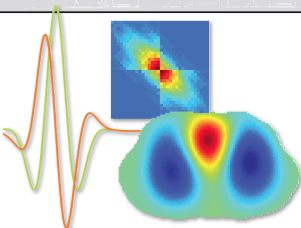
The VT device has been available in the international market since 2008.



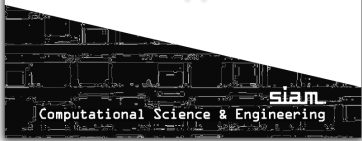
Here the CBCT reconstruction (right) gave 100 times more radiation than VT imaging (middle)



JENNIFER L. MUELLER • SAMULI SILTANEN



## Linear and Nonlinear Inverse Problems with Practical Applications



All Matlab codes freely available at this site!

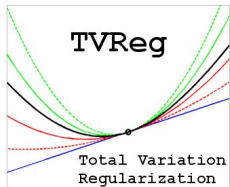
### Part I: Linear Inverse Problems

- 1 Introduction
- 2 Naïve reconstructions and inverse crimes
- 3 Ill-Posedness in Inverse Problems
- 4 Truncated singular value decomposition
- 5 Tikhonov regularization
- 6 Total variation regularization
- 7 Besov space regularization using wavelets
- 8 Discretization-invariance
- 9 Practical X-ray tomography with limited data
- 10 Projects

### Part II: Nonlinear Inverse Problems

- 11 Nonlinear inversion
- 12 Electrical impedance tomography
- 13 Simulation of noisy EIT data
- 14 Complex geometrical optics solutions
- 15 A regularized D-bar method for direct EIT
- 16 Other direct solution methods for EIT
- 17 Projects

## Another great resource is Per Christian Hansen's 3D tomography toolbox TVreg



**TVreg:** Software for 3D Total Variation Regularization (for Matlab Version 7.5 or later), developed by Tobias Lindstrøm Jensen, Jakob Heide Jørgensen, Per Christian Hansen, and Søren Holdt Jensen.

Website: <http://www2.imm.dtu.dk/~pcha/TVReg/>

# These books are recommended for learning the mathematics of practical X-ray tomography

1983 Deans: The Radon Transform and Some of Its Applications

1986 Natterer: The mathematics of computerized tomography

1988 Kak & Slaney: Principles of computerized tomographic imaging

1996 Engl, Hanke & Neubauer: Regularization of inverse problems

1998 Hansen: Rank-deficient and discrete ill-posed problems

2001 Natterer & Wübbeling: Mathematical Methods in Image Reconstruction

2008 Buzug: Computed Tomography: From Photon Statistics to Modern Cone-Beam CT

2008 Epstein: Introduction to the mathematics of medical imaging

2010 Hansen: Discrete inverse problems

2012 Mueller & S: Linear and Nonlinear Inverse Problems with Practical Applications

2014 Kuchment: The Radon Transform and Medical Imaging

# Outline

## Inverse problems and ill-posedness

### X-ray tomography

Mathematical model of X-ray attenuation

Tomographic imaging with sparse data

Regularized inversion

Industrial case study: low-dose 3D dental X-ray imaging

## Conclusion: linear and nonlinear inverse problems

# There are three main approaches for noise-robust solution of inverse problems

1. **Variational regularization.** Regularized solution is the minimizer of  $\|A(f) - m\|_Y^2 + \alpha\mathcal{R}(f)$ .
  - + The same code applies to many problems.
  - Repeated solution of direct problem needed.
  - Can get stuck in local minima.
2. **Problem-specific regularization.** Derive an analytical formula for recovering the unknown.
  - + Can deal efficiently with a specific nonlinearity.
  - Each formula applies to only one inverse problem.
3. **Bayesian inversion.** In the measurement equation  $m = A(x) + \varepsilon$ , model  $x, m, \varepsilon$  as random vectors. The solution is the *posterior distribution*  $\pi(x|m) = \pi(x)\pi(m|x)/\pi(m)$ .
  - + Very flexible framework, includes uncertainty quantification.
  - Computationally heavy.



Thank you for your attention!

# There are many computational approaches for computing the minimum

**Primal-dual algorithms** Chambolle, Chan, Chen, Esser, Golub, Mulet, Nesterov, Zhang

**Thresholding** Candès, Chambolle, Chaux, Combettes, Daubechies, Defrise, DeMol, Donoho, Pesquet, Starck, Teschke, Vese, Wajs

**Bregman iteration** Cai, Burger, Darbon, Dong, Goldfarb, Mao, Osher, Shen, Xu, Yin, Zhang

**Splitting approaches** Chan, Esser, Fornasier, Goldstein, Langer, Osher, Schönlieb, Setzer, Wajs

**Nonlocal TV** Bertozzi, Bresson, Burger, Chan, Lou, Osher, Zhang

We found that **quadratic programming** works well for us.

# Quadratic programming (QP) for TV regularization

The minimizer of the functional

$$\arg \min_{f \in \mathbb{R}_+^n} \left\{ \|Af - m\|_2^2 + \alpha \|L_H f\|_1 + \alpha \|L_V f\|_1 \right\}$$

can be transformed into the standard form

$$\arg \min_{z \in \mathbb{R}^{5n}} \left\{ \frac{1}{2} z^T Q z + c^T z \right\}, \quad z \geq 0, \quad E z = b,$$

where  $Q$  is symmetric and  $E$  implements equality constraints.

Large-scale primal-dual interior point QP method was developed in Kolehmainen, Lassas, Niinimäki & S (2012) and Hämäläinen, Kallonen, Kolehmainen, Lassas, Niinimäki & S (2013).

$$\text{Reduction to } \arg \min_{z \in \mathbb{R}^{5n}} \left\{ \frac{1}{2} z^T Q z + c^T z \right\}$$

Denote horizontal and vertical differences by

$$L_H f = u_H^+ - u_H^- \quad \text{and} \quad L_V f = u_V^+ - u_V^-,$$

where  $u_H^\pm, u_V^\pm \geq 0$ . TV minimization is now

$$\arg \min_{f \in \mathbb{R}_+^n} \left\{ f^T A^T A f - 2f^T A^T m + \alpha \mathbf{1}^T (u_H^+ + u_H^- + u_V^+ + u_V^-) \right\},$$

where  $\mathbf{1} \in \mathbb{R}^n$  is vector of all ones. Further, we denote

$$z = \begin{bmatrix} f \\ u_H^+ \\ u_H^- \\ u_V^+ \\ u_V^- \end{bmatrix}, \quad Q = \begin{bmatrix} \frac{1}{\sigma^2} A^T A & 0 & 0 & 0 & 0 \\ 0 & 0 & 0 & 0 & 0 \\ 0 & 0 & 0 & 0 & 0 \\ 0 & 0 & 0 & 0 & 0 \\ 0 & 0 & 0 & 0 & 0 \end{bmatrix}, \quad c = \begin{bmatrix} -2A^T m \\ \alpha \mathbf{1} \\ \alpha \mathbf{1} \\ \alpha \mathbf{1} \\ \alpha \mathbf{1} \end{bmatrix}.$$

## Projected Barzilai-Borwein minimization

For  $f \in \mathbb{R}^n$ , denote  $\|f\|_\beta := \sum_{i=1}^n \sqrt{(f_i)^2 + \beta}$ , with a small parameter  $\beta > 0$ . We minimize

$$G_\beta(f) := \frac{1}{2} \|Af - \tilde{\mathbf{g}}\|_2^2 + \alpha (\|L_H f\|_\beta + \|L_V f\|_\beta),$$

with a non-negativity constraint:

$$f^{k+1} = P \left( f^k - \lambda_k \nabla G_\beta(f^k) \right), \quad k = 0, \dots, k_{max} - 1.$$

The step size is

$$\lambda_k = \frac{(f^k - f^{k-1})^T (f^k - f^{k-1})}{(f^k - f^{k-1})^T (\nabla G_\beta(f^k) - \nabla G_\beta(f^{k-1}))}$$

and  $P : \mathbb{R}^n \rightarrow \mathbb{R}^n$  is the projection

$$(P(f))_i = \begin{cases} f_i & \text{if } f_i \geq 0 \\ 0 & \text{if } f_i < 0 \end{cases}, \quad i = 1, \dots, n.$$